Fulcrum Therapeutics

Discovery of clinical candidate FTX-6058:
a potent, orally bioavailable upregulator of fetal hemoglobin for treatment of sickle cell disease

2021 Spring ACS National Meeting

Ivan V. Efremov,* Kingsley Kofi Appiah, Angela Cacace, Yanfei Dong, Shawn D. Johnstone, Steven Kazmirski, Qingyi Li, Christopher Moxham, Peter Rahl, Mark Roth, Billy Stuart, Lorin A. Thompson, III, Owen B. Wallace, Keqiang Xie, Feng Zhou

Disclaimer

- Ivan Efremov is a full time, paid employee of Fulcrum Therapeutics and owns restricted stock and/or stock options in Fulcrum Therapeutics.
- Any opinions expressed are his and may or may not be consistent with Fulcrum Therapeutics perspective.
- Any forward-looking statements are based on current expectations of future events and are subject to a number of risks and uncertainties that could cause actual results to differ materially and adversely from those set forth in, or implied by, such forward-looking statements.

Fulcrum overview

Clinical stage biopharmaceutical company using systematic approach to identify small molecules able to rebalance gene expression

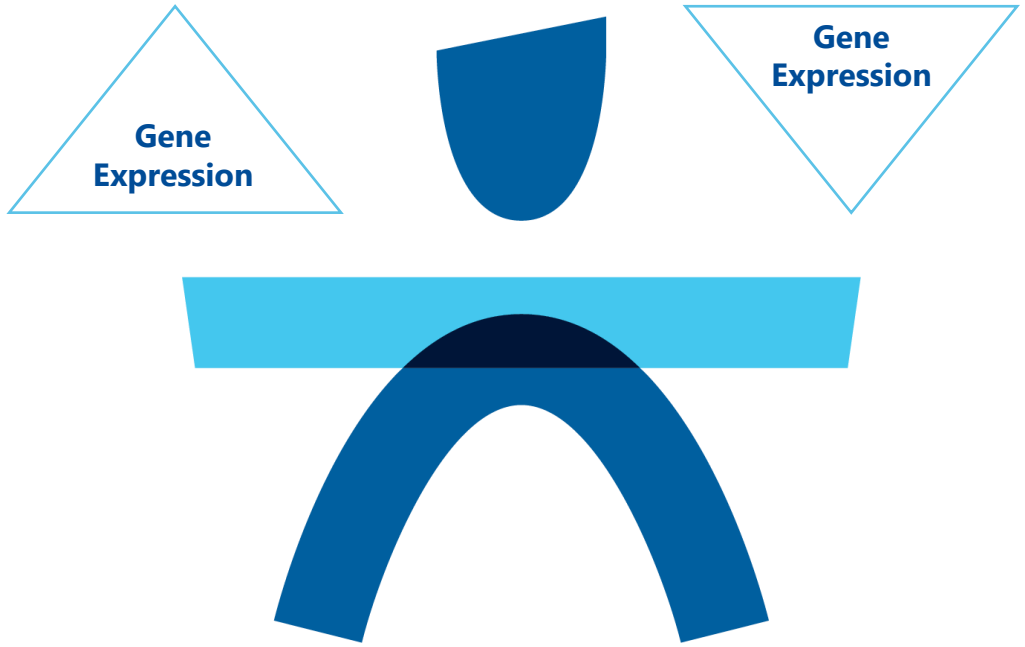

- ~7,000 genetically defined diseases today
- We are building on decades of research highlighting gene expression role in disease
- High-throughput product engine designed to rapidly identify and validate drug targets that can modulate gene expression and treat disease at its root cause
- Focus on small molecules as therapeutic modality

Our vision is to treat genetically defined diseases by addressing their root cause

Fulcrum comprehensively interrogates diseases to identify points of intervention & accelerate discovery of disease modifying therapies

Intelligent drug discovery in disease relevant models through high dimensional data and machine learning

Discovery Engine

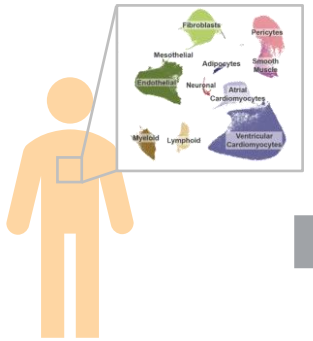

Insights from proprietary and public clinical samples / datasets

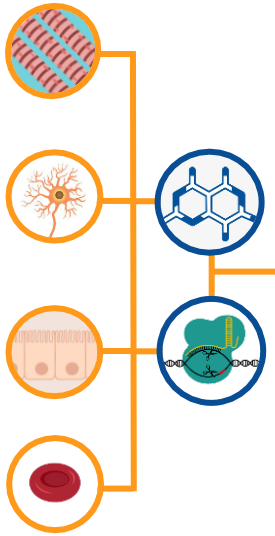

Disease relevant cell models interrogated with small molecules, RNAi and CRISPR

Computational Engine

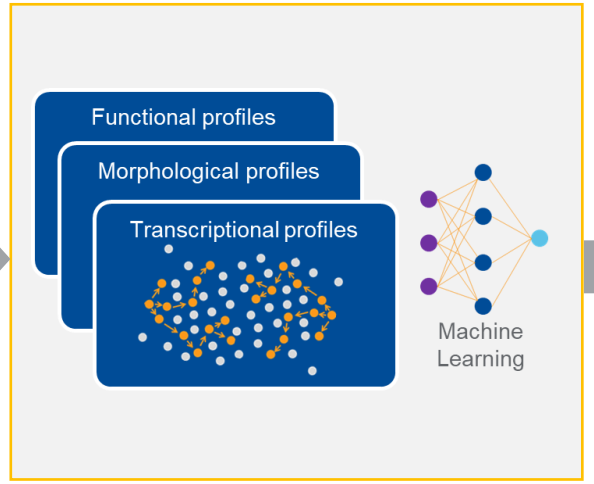

Machine Learning on high dimensional transcriptomic and imaging data enables insights into target and disease biology

Accelerated Drug Discovery Programs

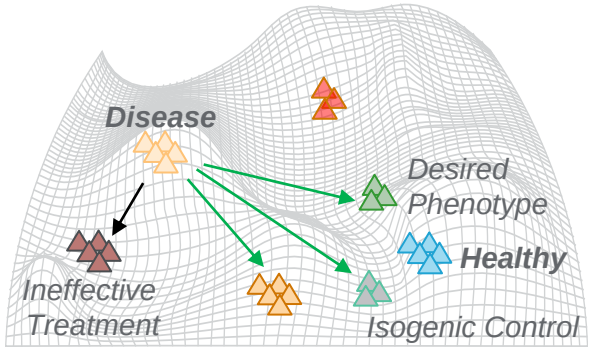

Highly de-risked target and development candidates

- ✓ **Targets with specificity, selectivity and tolerability**
- ✓ **Tissue-relevant translatable biomarkers**
- ✓ **Foresight on potential toxicity or off-target activity**

SCD is caused by mutations in adult hemoglobin gene

- Adult hemoglobin (HbA) is a tetrameric complex of two alpha chains and two beta chains – a2b2
- SCD is caused by a mutation within the HBB gene that encodes the adult b-globin subunit
- The resulting HbS undergoes polymerization in the deoxygenated state
- Fetal hemoglobin is a functional paralog that is produced in development

Image from the RCSB PDB (rcsb.org) of 6BB5 (J.R. Terrell, R.H.Gumpper, M. Luo (2018) Hemoglobin crystals immersed in liquid oxygen reveal diffusion channels Biochem Biophys Res Commun 495: 1858-1863).

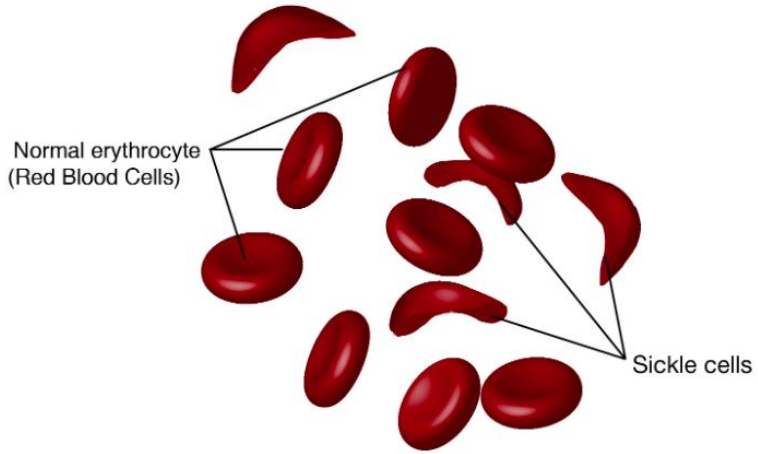

Image from: https://www.genome.gov/genetics-glossary/Sickle-Cell-Disease

Human hemoglobin during development

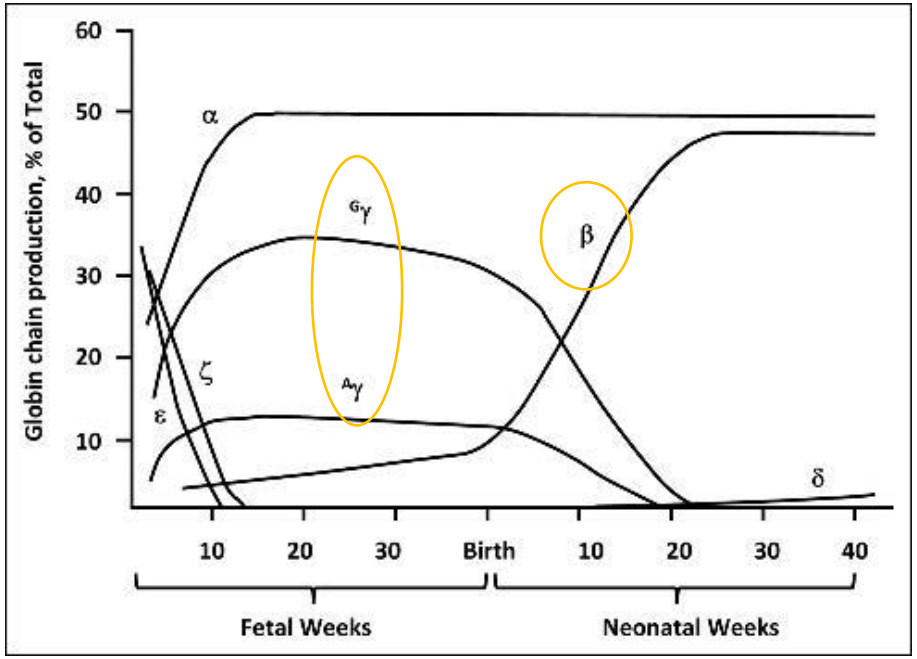

ε – embryonic hemoglobin
γ – fetal hemoglobin
β, δ – adult hemoglobin

HbF mitigates mortality and morbidity risks associated with sickle cell disease

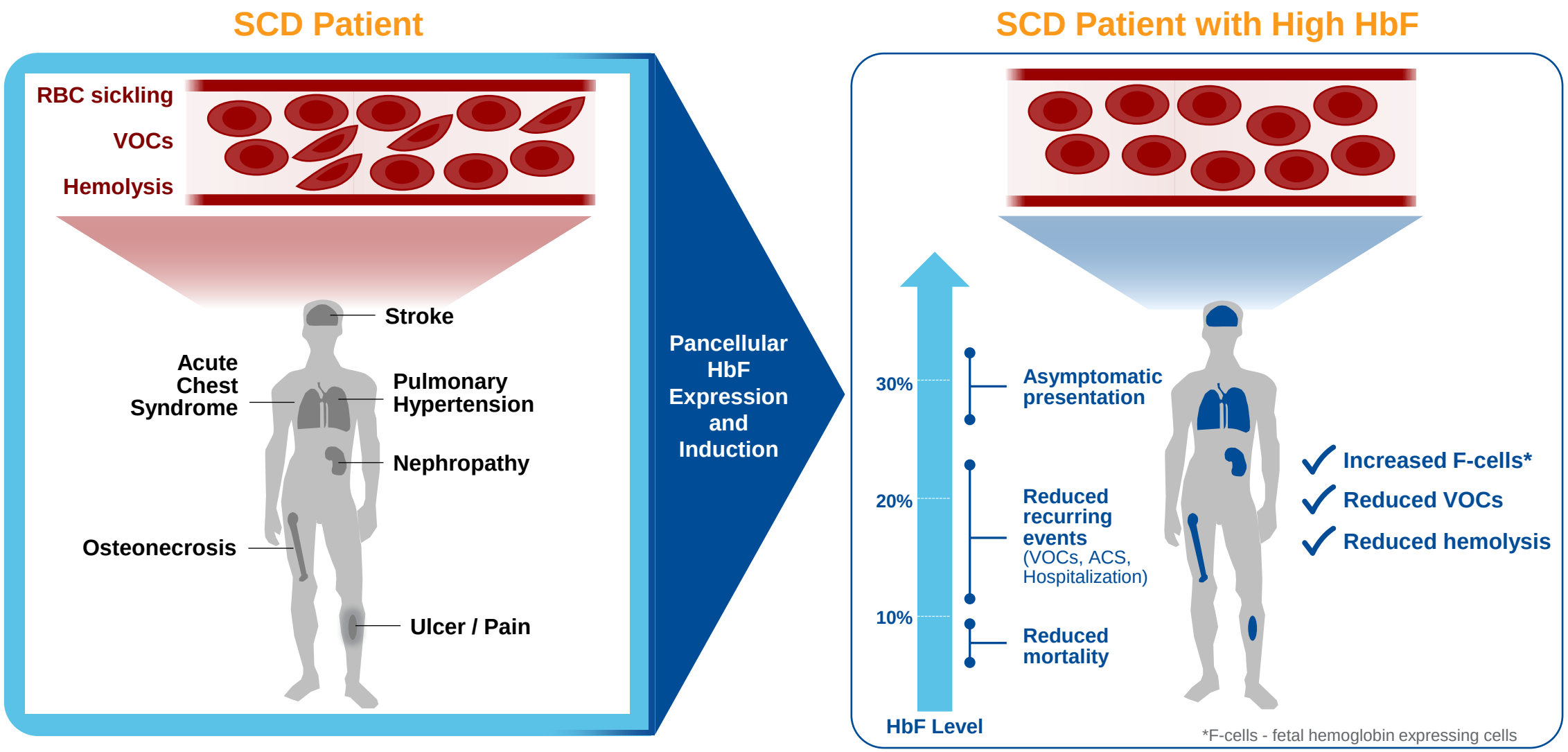

Powars, DR. Blood. 1984; Estepp, JH. Br J Haematol. 2013; Platt, OS. NEJM. 1994; Akinsheye, I. Blood. 2011.

Lead target identified using multiple approaches

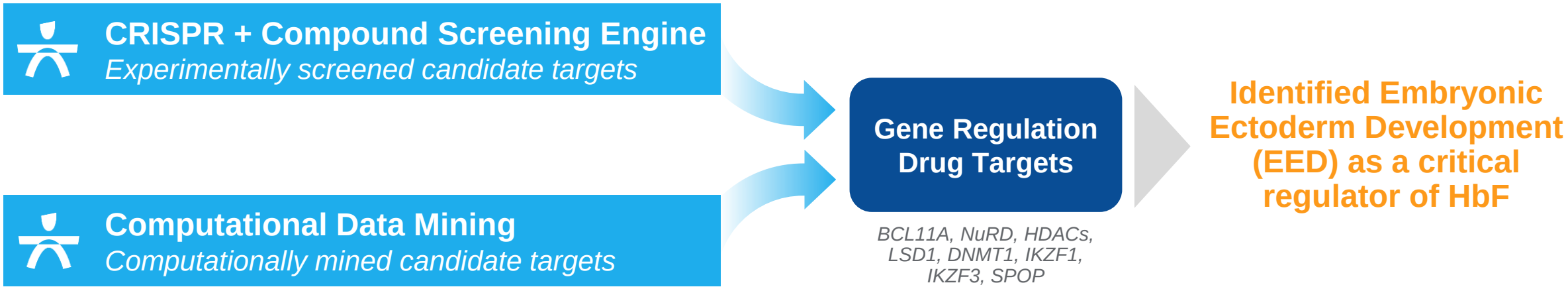

- Screen in HUDEP2 erythroid progenitor cells
- Multiple target candidates identified
- Chemical probe and CRISPR screens converged on PRC2 complex
- EED was selected for novel Fulcrum chemistry focus

Allosteric regulation of PRC2 activity

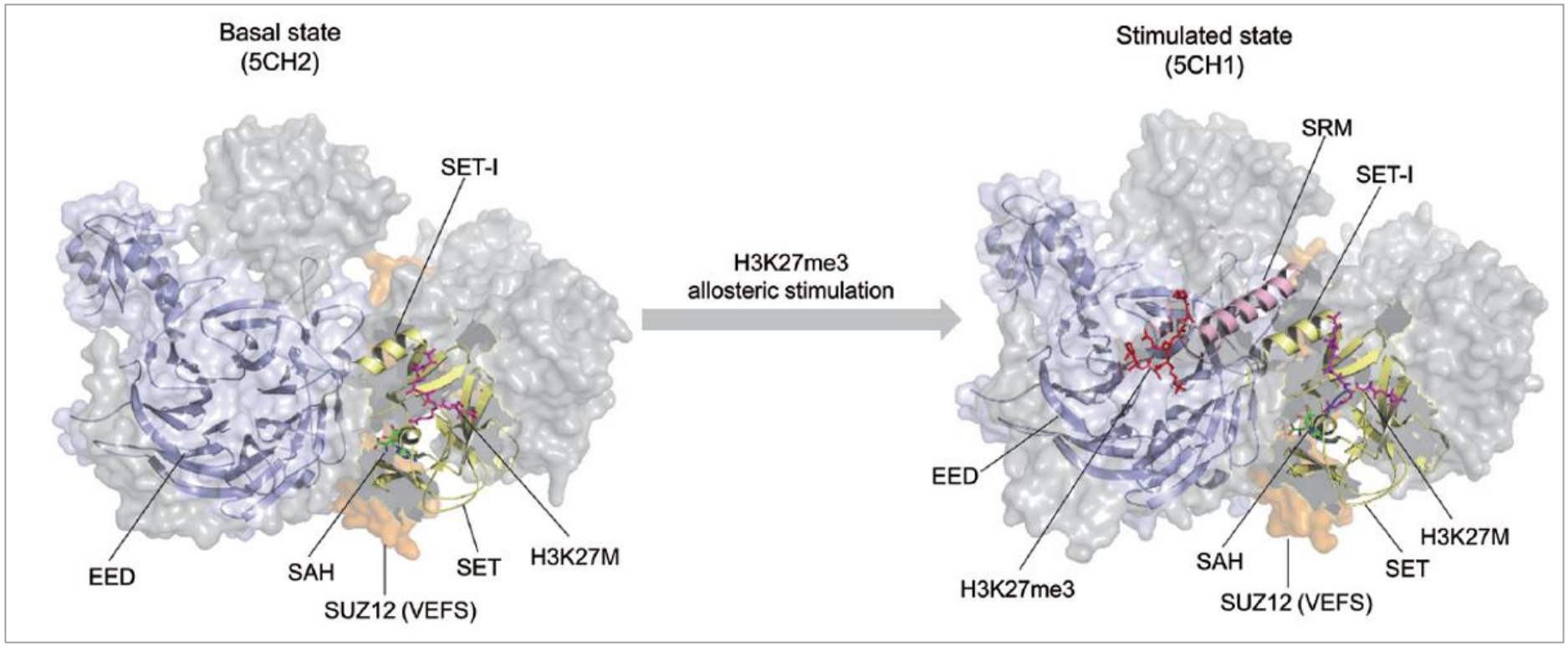

Adapted from: Yi Shi *et al.*, "Structure of the PRC2 complex and application to drug discovery" *Acta Pharmacol. Sinica* **2017**, 963-976.

- PRC2 complex catalyzes tri-methylation of H3K27, leading to nucleosome compaction and transcription silencing
- The flexible stimulation-responsive motif (SRM helix) of EZH2 is disordered in the basal state of the PRC2 ternary complex
- EED-bound H3K27me3 peptide interaction with the SRM induces its structure resulting in binding to the catalytic SET-I domain of EZH2
- Rotation of SET-I and opening of the substrate-binding cleft result in stimulation of the PRC2 activity
- FTX-6058 selectively binds EED, resulting in inhibition of PRC2 activity and increases in *HBG1/2* gene expression (encoding HbF)

EED ligands reported in the literature as of 2017

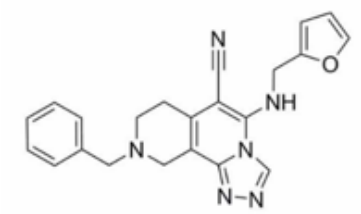

EED162 [2,4]

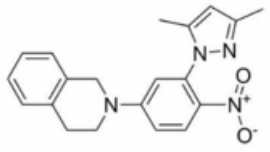

EED666 [4]

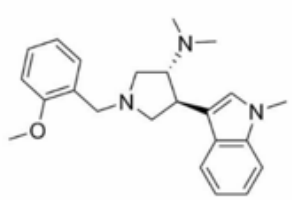

EED709 [1,4]

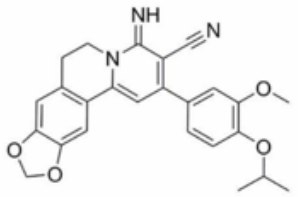

EED396 [4]

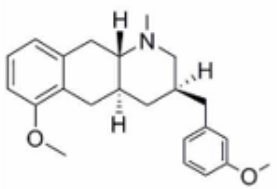

EED210 [4]

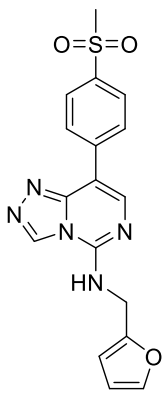

EED226 [2,4]

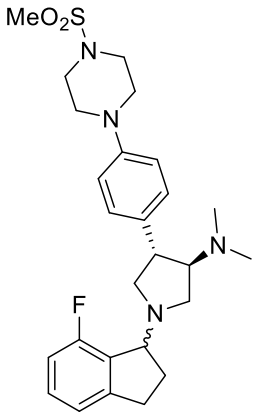

A-395 [1,3]

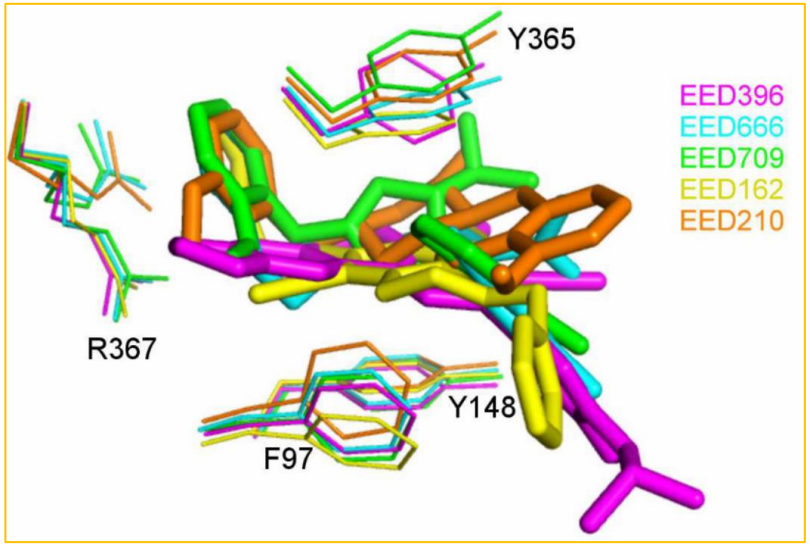

Adapted from L. Li *et al.* PLoS ONE **12** (*4*), e0169855.

[1] M. L. Curtin *et al.* Bioor. Med. Chem. Lett. *2017*, **27** (*7*), 1576-83.

[2] Y. Huang *et al.* J. Med. Chem. *2017*, **60**, 2215-26.

[3] Y. He *et al.* Nat. Chem. Biol. *2017*, **13** (*4*), 385-395.

[4] L. Li *et al.* Nat. PLoS ONE **12** (*4*), e0169855.

Key features of the EED binding site

EED226 bound to EED

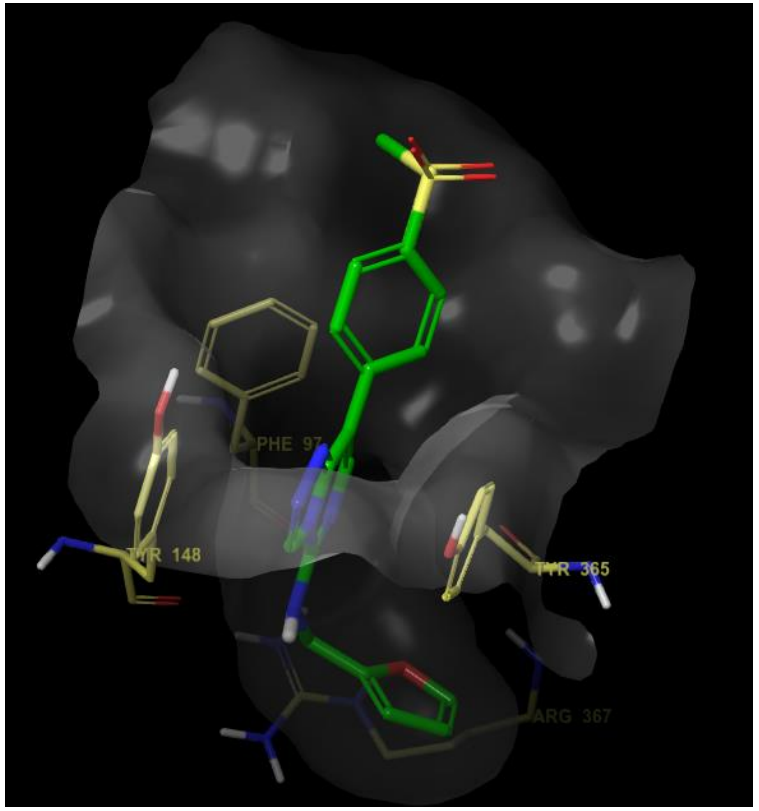

Image of 5GSA (W. Qi *et al.*, (2017) An allosteric PRC2 inhibitor targeting the H3K27me3 binding pocket of EED Nature Chem. Biol. 13: 381-388) created using Maestro (Schrodinger).

- Aromatic cage as a recognition element for trimethylated lysine
- Electron-deficient Arg on the bottom of the binding site
- 3 electron-rich Ar rings (Phe97, Tyr148, Tyr365) form the “walls” of the aromatic cage
- Modification of the solvent-exposed substituent can result in potency improvement
- The central core motifs of known EED binders broadly fall in two categories:
  - Those with a positive charge
  - Neutral compounds with e-deficient Ar rings

Medicinal chemistry strategy

- Agnostic to the origin of chemical matter: VS, FBLG, de novo design, literature tools – all approaches provided hits
- Eventually, a decision to focus on neutral core binders
- Comparative analysis of different cores
- Parallel chemistry to scope out the head group
- Map out productive occupancy of the deep pocket
- Rigidify the binding conformation

Medicinal chemistry strategy

- Agnostic to the origin of chemical matter: VS, FBLG, de novo design, literature tools – all approaches provided hits
- Eventually, a decision to focus on neutral core binders
- Comparative analysis of different cores
- Parallel chemistry to scope out the head group
- Map out productive occupancy of the deep pocket
- Rigidify the binding conformation

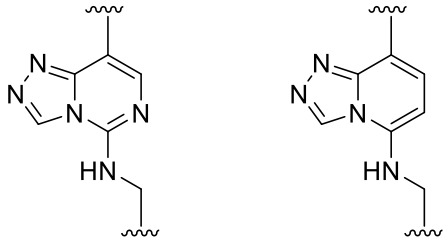

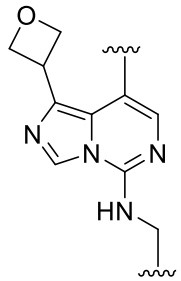
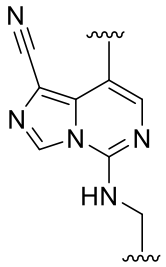
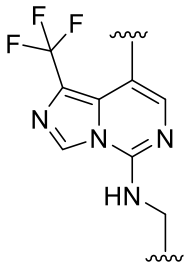
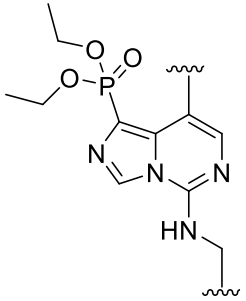
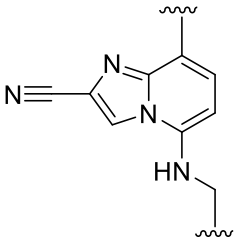

Medicinal chemistry strategy

- Agnostic to the origin of chemical matter: VS, FBLG, de novo design, literature tools – all approaches provided hits
- Eventually, a decision to focus on neutral core binders
- Comparative analysis of different cores
- Parallel chemistry to scope out the head group
- Map out productive occupancy of the deep pocket
- Rigidify the binding conformation

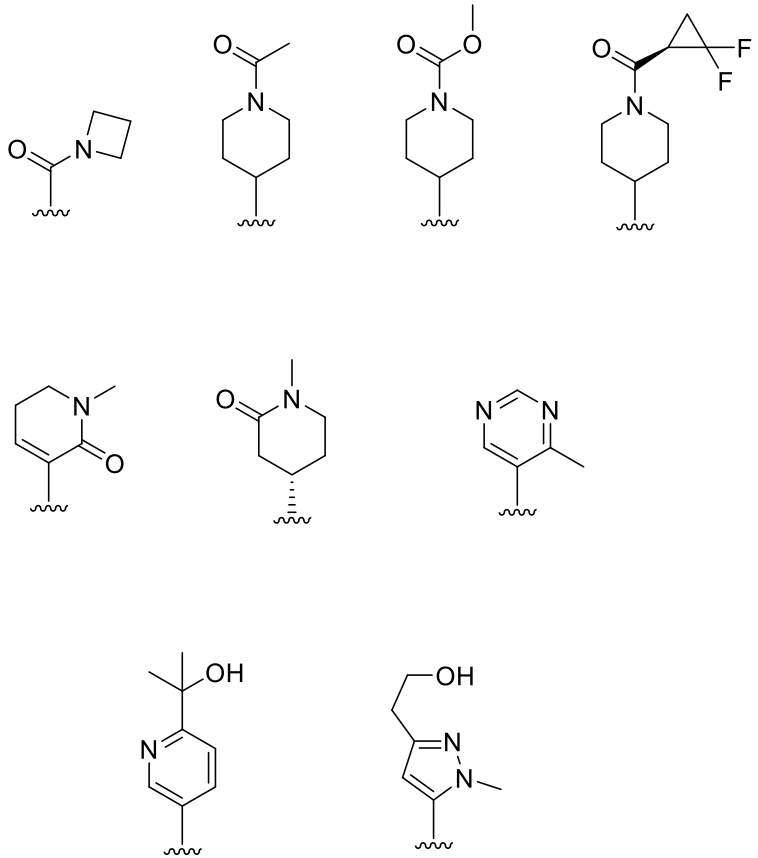

Medicinal chemistry strategy

- Agnostic to the origin of chemical matter: VS, FBLG, de novo design, literature tools – all approaches provided hits
- Eventually, a decision to focus on neutral core binders
- Comparative analysis of different cores
- Parallel chemistry to scope out the head group
- Map out productive occupancy of the deep pocket
- Rigidify the binding conformation

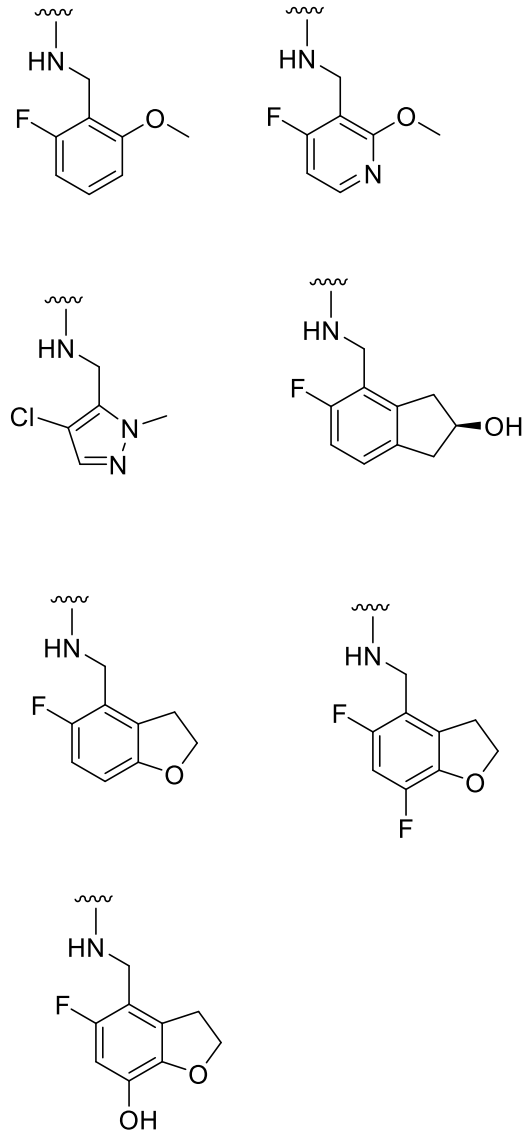

Medicinal chemistry strategy

- Agnostic to the origin of chemical matter: VS, FBLG, de novo design, literature tools – all approaches provided hits
- Eventually, a decision to focus on neutral core binders
- Comparative analysis of different cores
- Parallel chemistry to scope out the head group
- Map out productive occupancy of the deep pocket
- Rigidify the binding conformation

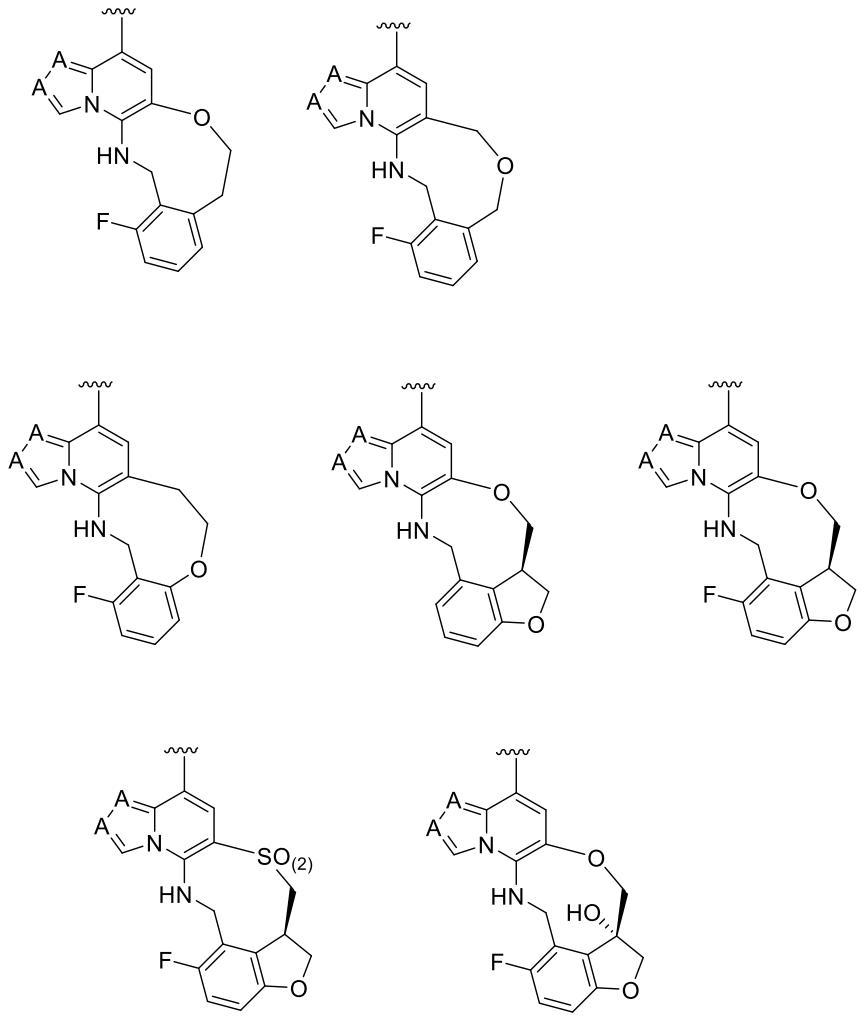

Early on, promising leads were identified in the azolopyrimidine series

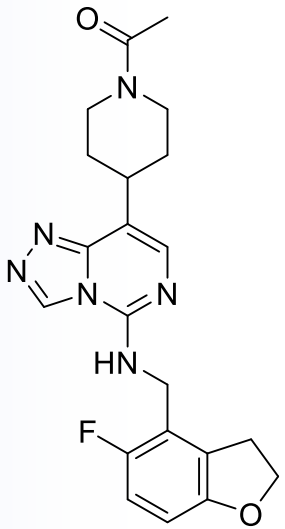

EED K_D (SPR) = 1.8 nM
biochemical IC_{50} (PRC2) = 6.8 nM
H3K27me3 IC_{50} (P-gp HEK) = 200 nM
H3K27me3 IC_{50} (CD34+) = 64 nM
LogD (pH 7.4) = 2.2
MDCK AB = 2.9 x 10^{-6} cm/s
HLM Clint < 9.6 uL/min/mg

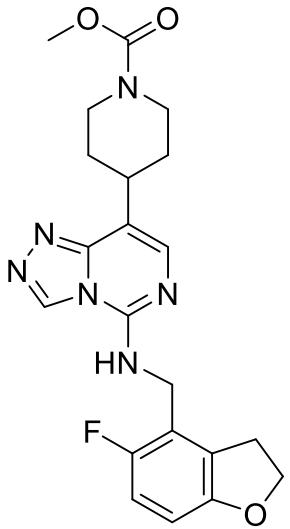

EED K_D (SPR) = 3.2 nM
biochemical IC_{50} (PRC2) = 5.0 nM
H3K27me3 IC_{50} (P-gp HEK) = 77 nM
H3K27me3 IC_{50} (CD34+) = 300 nM
LogD (pH 7.4) = 3.1
MDCK AB = 29 x 10^{-6} cm/s
HLM Clint = 18 uL/min/mg

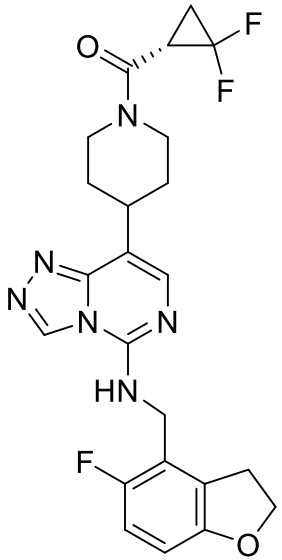

EED K_D (SPR) = 0.69 nM
biochemical IC_{50} (PRC2) = 3.2 nM
H3K27me3 IC_{50} (P-gp HEK) = 30 nM
H3K27me3 IC_{50} (CD34+) = 20 nM
LogD (pH 7.4) = 3.1
MDCK AB = 5.9 x 10^{-6} cm/s
HLM Clint = 142 uL/min/mg

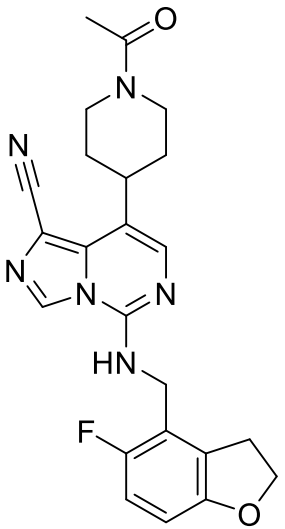

EED K_D (SPR) = 0.80 nM
biochemical IC_{50} (PRC2) = 3.9 nM
H3K27me3 IC_{50} (P-gp HEK) = 43 nM
H3K27me3 IC_{50} (CD34+) = 40 nM
LogD (pH 7.4) = 3.24
MDCK AB = 13 x 10^{-6} cm/s
HLM Clint = 41 uL/min/mg

- **Identification of nonaromatic solvent-exposed substituents looked promising**
- **However, a desired balance of potency and DMPK parameters was difficult to realize**
- **A different solution was required**

Potential advantages of the macrocyclization approach

- Minimizing the entropic penalty of flexible ligands upon binding event
- Decreasing potential for off-target interactions by limiting the number of possible conformations
- Opportunity to enhance resistance in oncology and infectious diseases
- Potential for lower clearance due to decreased sampling of conformations recognized by metabolic enzymes
- In principle, cyclization could lead to improved permeability due to more globular shape and preorganization of polar functionalities
- Modulation of tissue partitioning such as CNS accessibility
- But: synthesis can be complicated, and it is not easy to recapitulate the binding conformation

- M. D. Cummings, S. Sekharan **J. Med. Chem.** *2019*, **62** (*15*), 6843-53.
- J. Mallinson, I. Collins **Future Med. Chem.** *2012*, **4** (*11*), 1409-38.
- **Practical Medicinal Chemistry with Macrocycles: Design, Synthesis, and Case Studies,** Ed. by E. Marsault, M. L. Peterson, John Wiley & Sons, Inc., 2017.
- T. W. Johnson *et al.* **J. Med. Chem.** *2014*, **57** (*11*), 4720-44.

Prioritization of macrocyclic ideas for synthesis

20 intramolecular cyclization ideas were triaged by analysis of multiple docked poses in multiple crystal structures (hydrated and unhydrated), *e.g:*

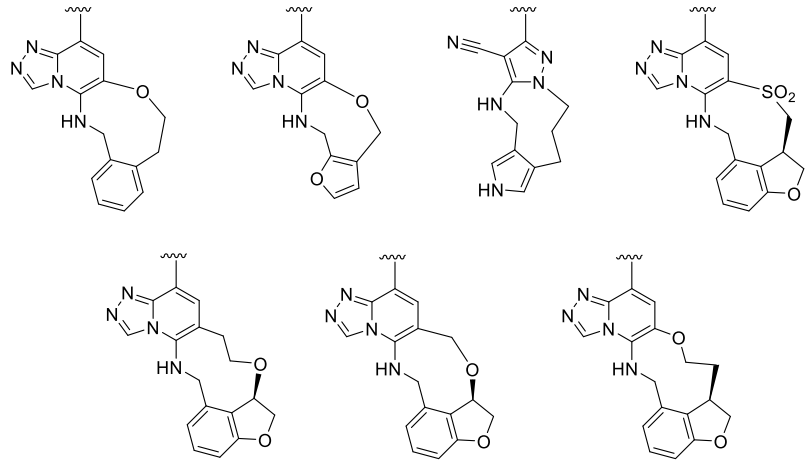

4 scaffolds looked more promising based on the poses, predicted protein-ligand interactions, and docking scores

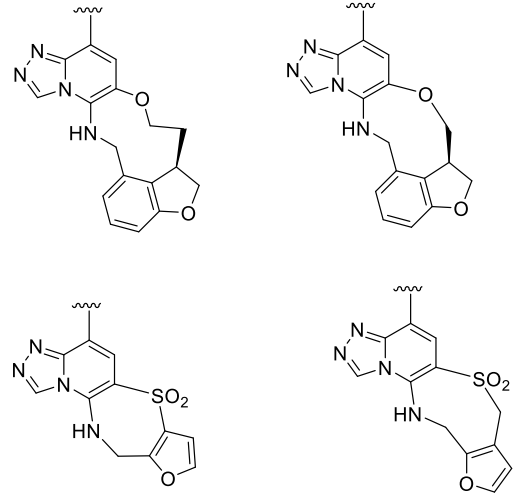

1 scaffold looked by far the best recapitulating the binding pose of the nonmacrocyclic leads

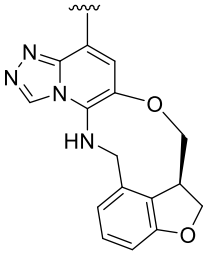

Initial route to macrocyclic analogs: synthesis and coupling of key intermediates

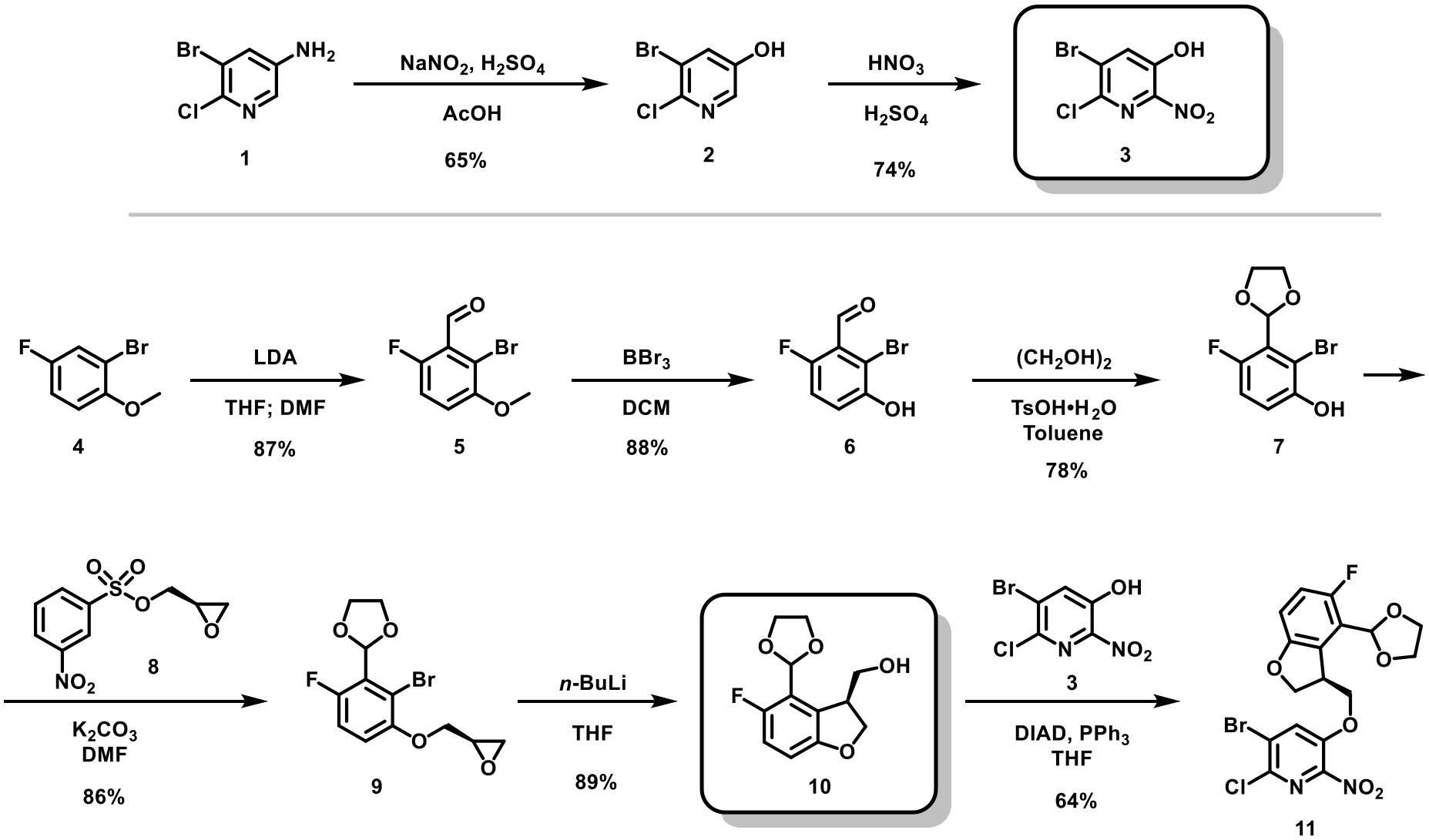

Initial route to macrocyclic analogs: 1st generation macrocyclization approach

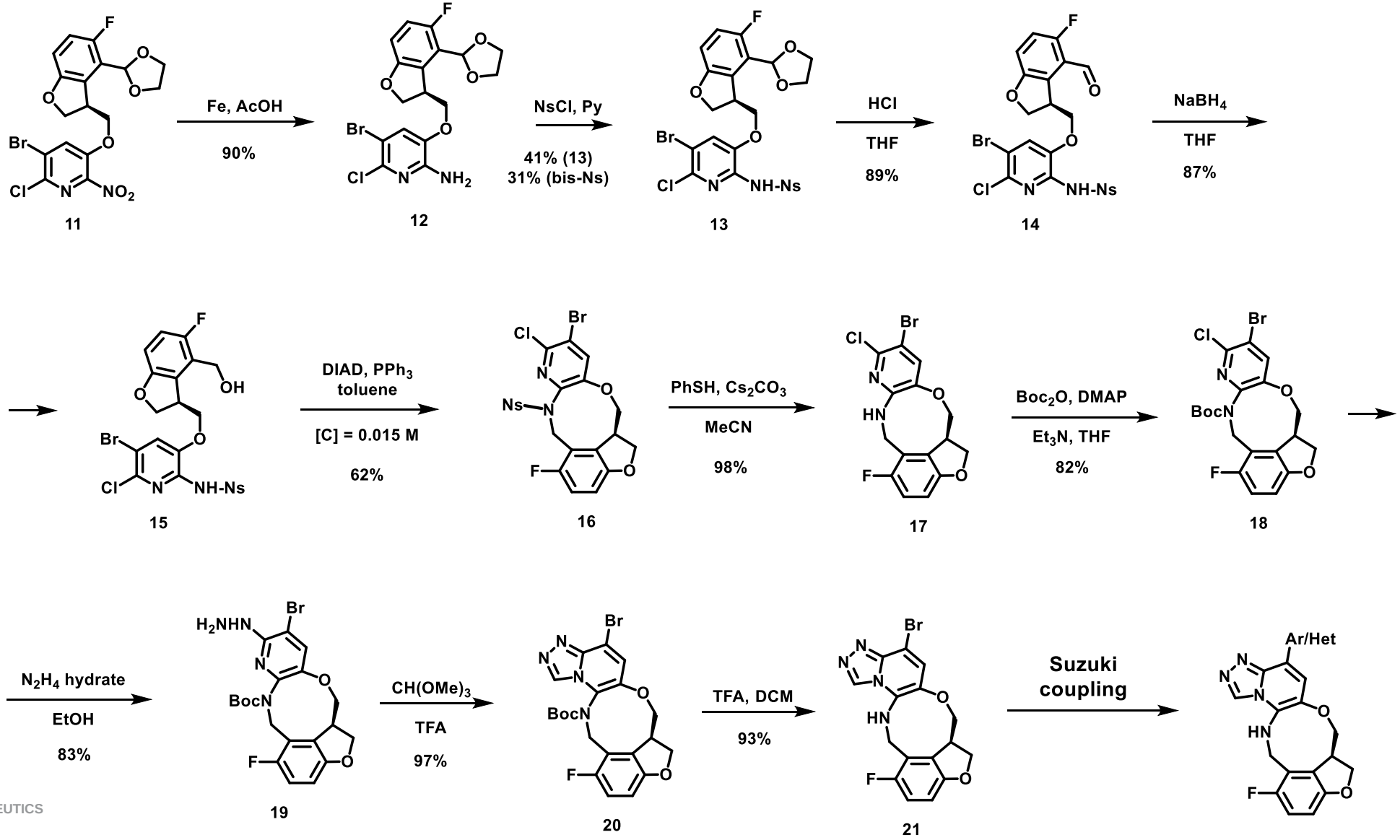

Structural observations for the designed macrocyclic analog

Overlap of bound (green; 2.25Å resolution) and docked (white) poses of the designed analog

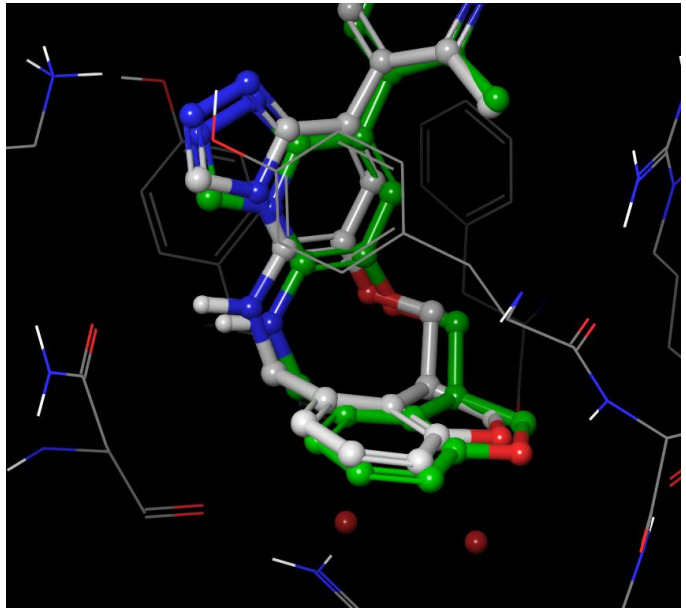

- Experimental pose matched the predicted one very well

X-ray overlap of the macrocyclic analog with EED226 (5GSA structure)

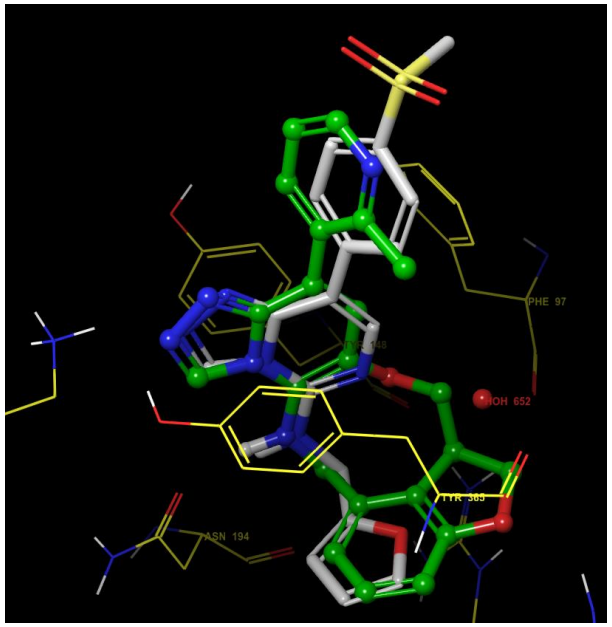

- Binding mode maintained
- Larger deep pocket substituent leads to rotation of Arg-367 and displacement of not fully coordinated water molecule

Overlap of X-ray structures of the macrocyclic and nonmacrocyclic analogs

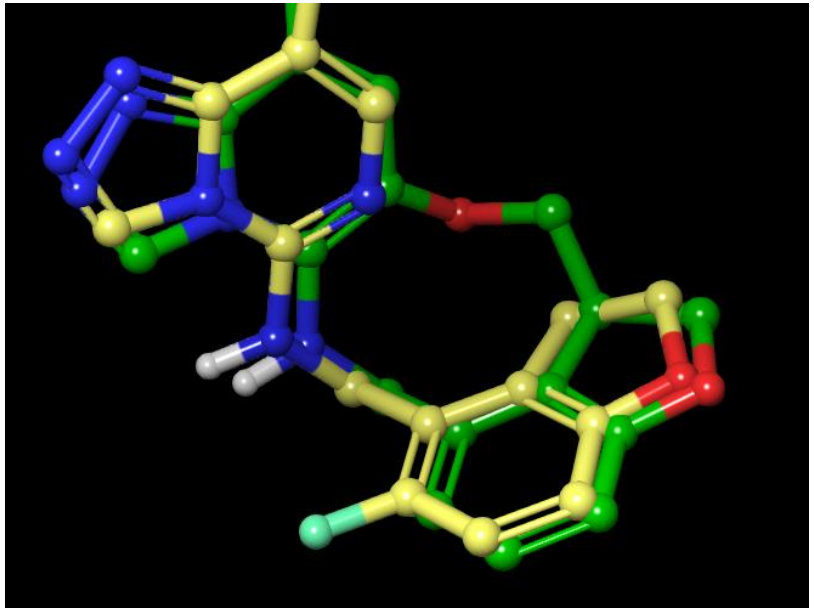

- Designed macrocycle recapitulated the bound conformation of the nonmacrocyclic analogs
- Nearly identical occupancy of the binding site

Macrocyclization led to consistent affinity improvement

Pairwise analysis - SPR KD

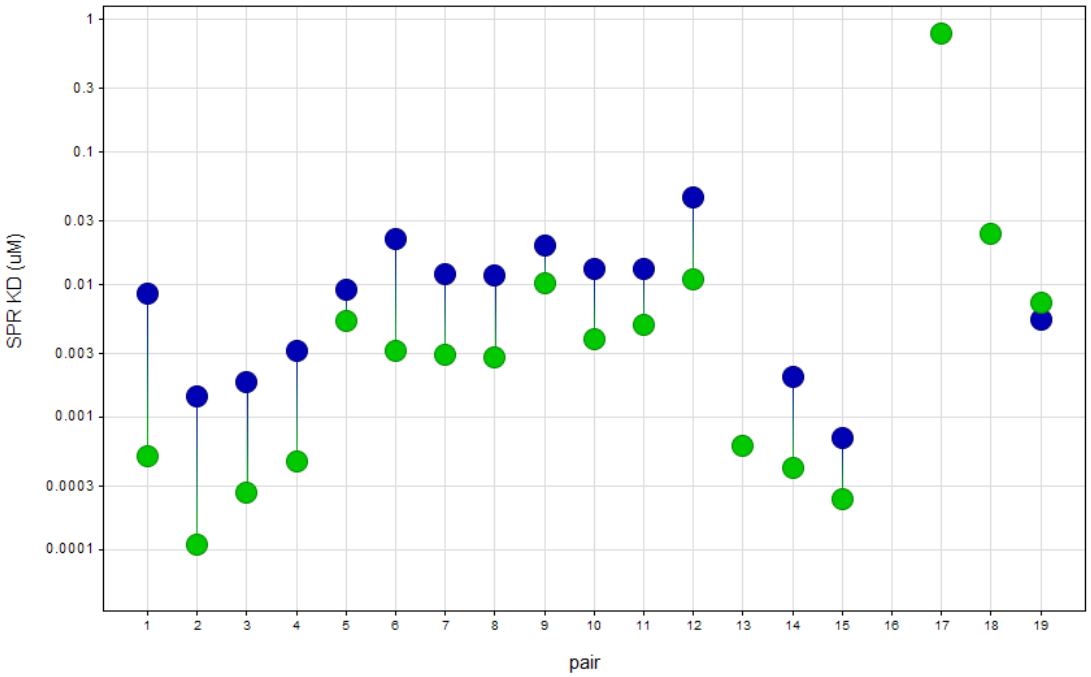

Pairwise analysis – LipE values (SPR K_D, calculated LogP)

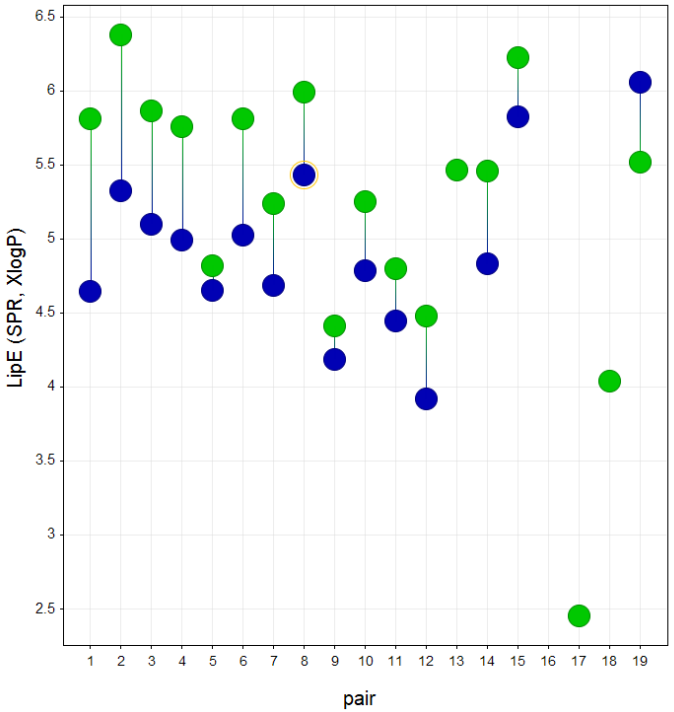

Pairwise analysis – LipE values (SPR K_D, measured LogD at pH=7.4)

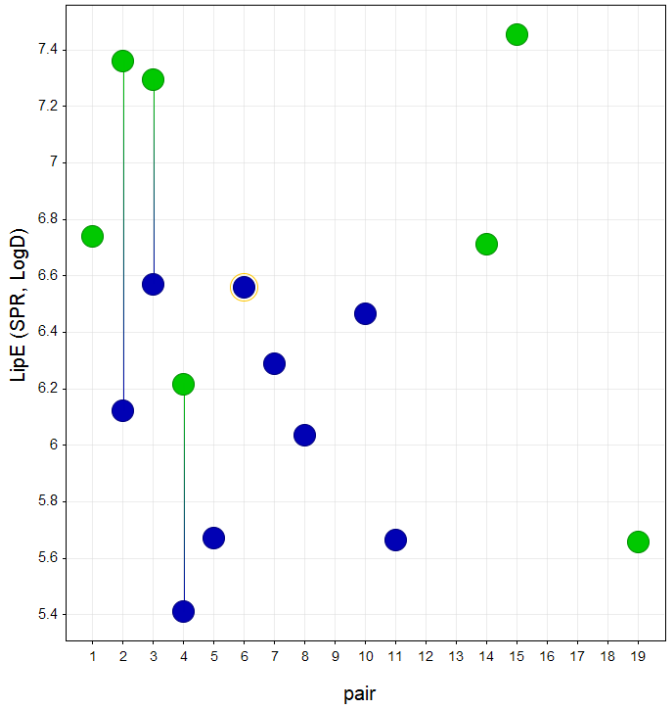

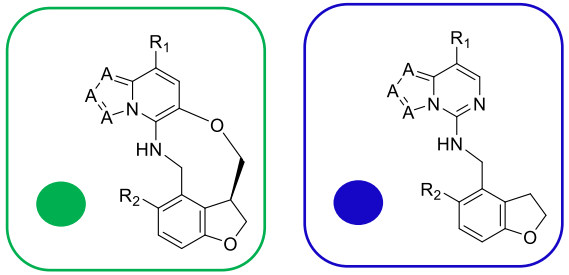

Macrocyclic analogs within matched pairs exhibited consistently stronger binding to EED, in an absolute sense and when corrected for lipophilicity.

Key SAR trends and observations

para-substitution can improve potency but should be small for adequate DMPK profile

ortho-substitution preferred for potency

substitution of the imidazole ring can improve potency but is LipE-neutral and may lead to higher clearance

F is the optimal substituent for cell potency and DMPK

5- and 6-heteroaryls offer best balance of potency and DMPK

- preferred position for the O atom
- O preferred to S, SO_2

R5 could be OH to pick up interactions with polar environment at the bottom of the deep pocket

dihydrofuran ring is optimal for occupancy of the deep pocket

F or OH can be used to productively fill a small pocket

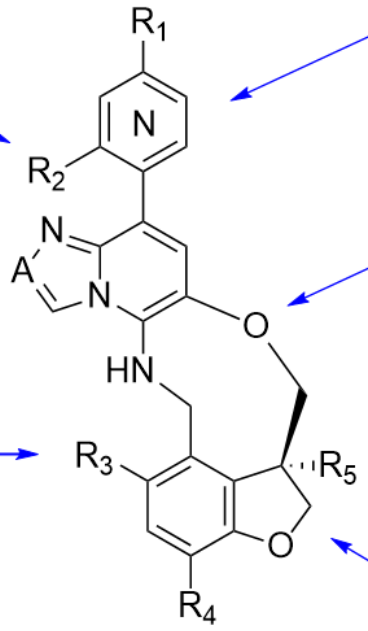

Development candidate ID as the result of multiparameter optimization

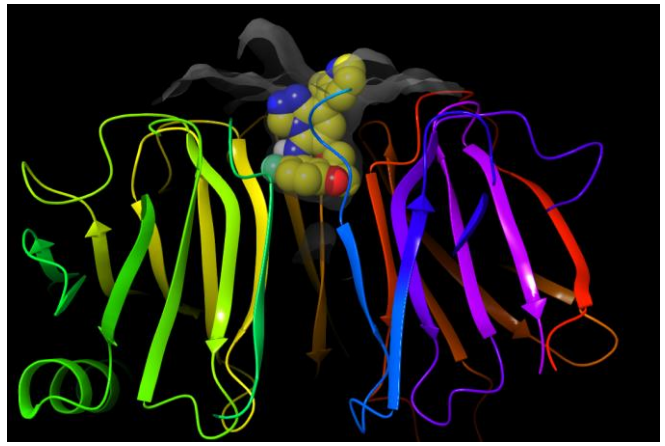

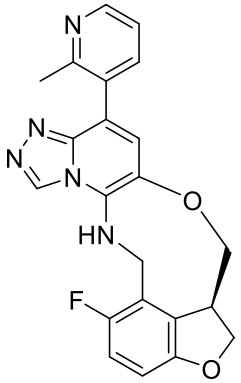

FTX-6058

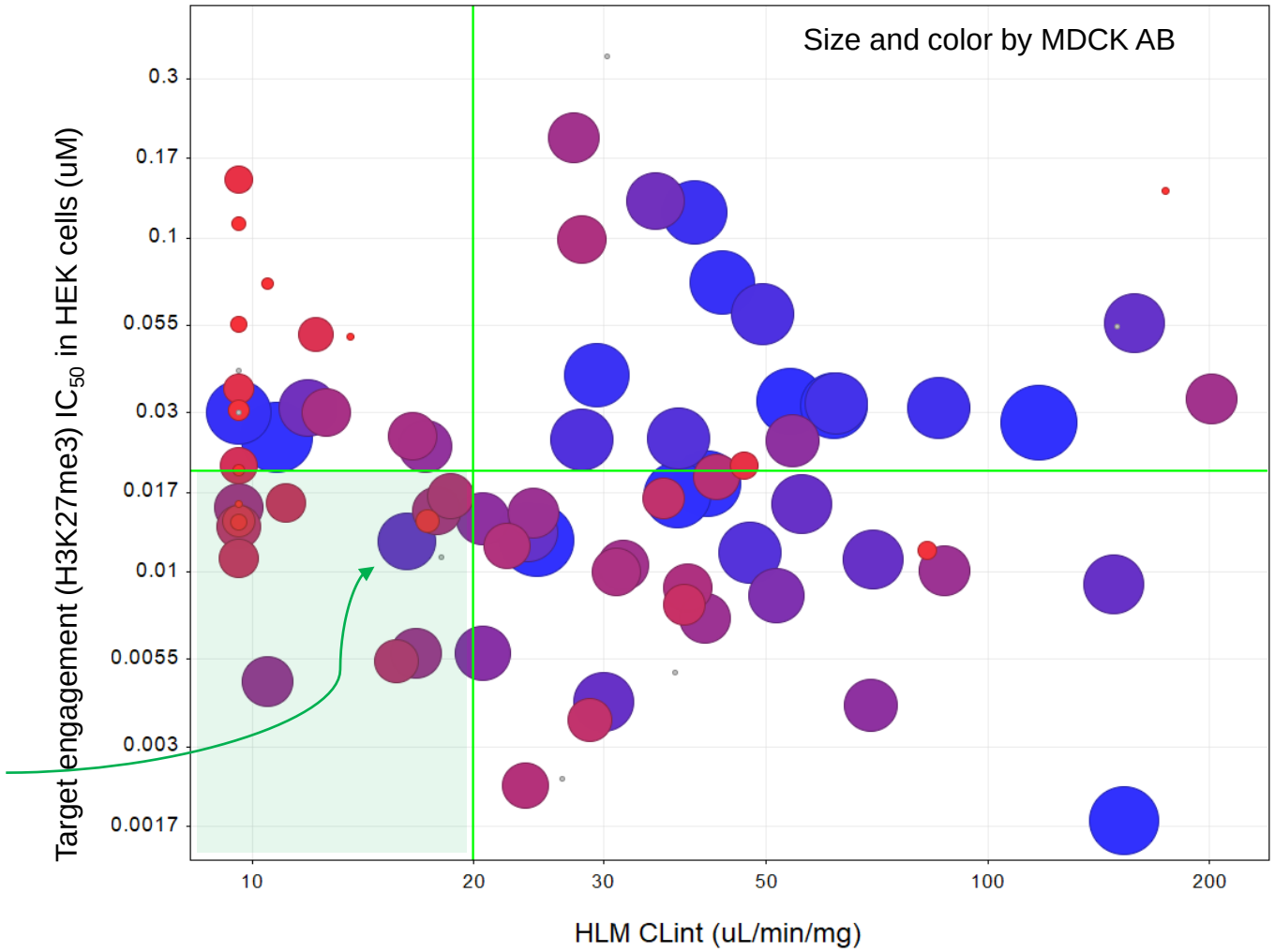

Optimized discovery route to FTX-6058: cyclization and the end game

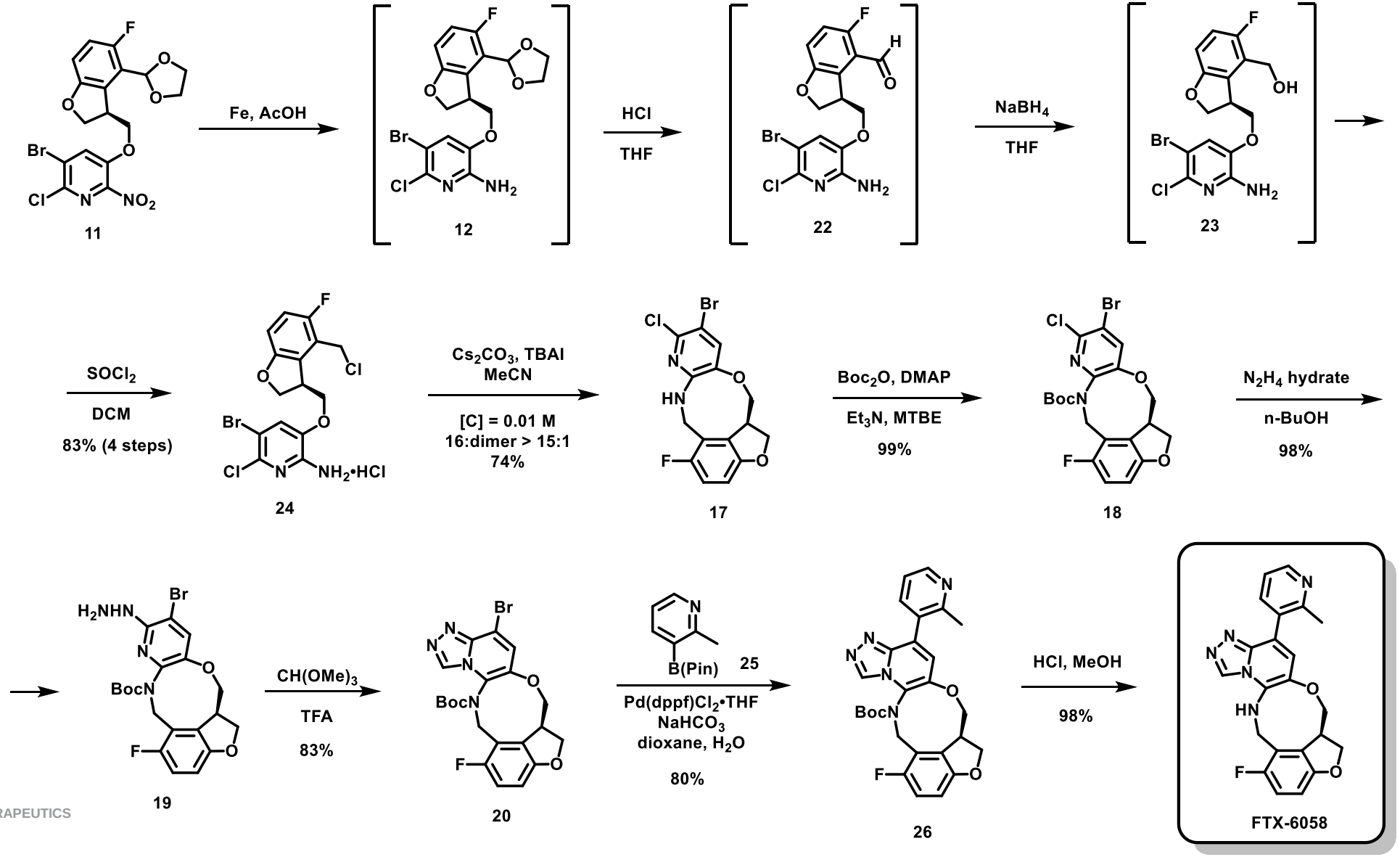

Screening funnel and FTX-6058 *in vitro* profile

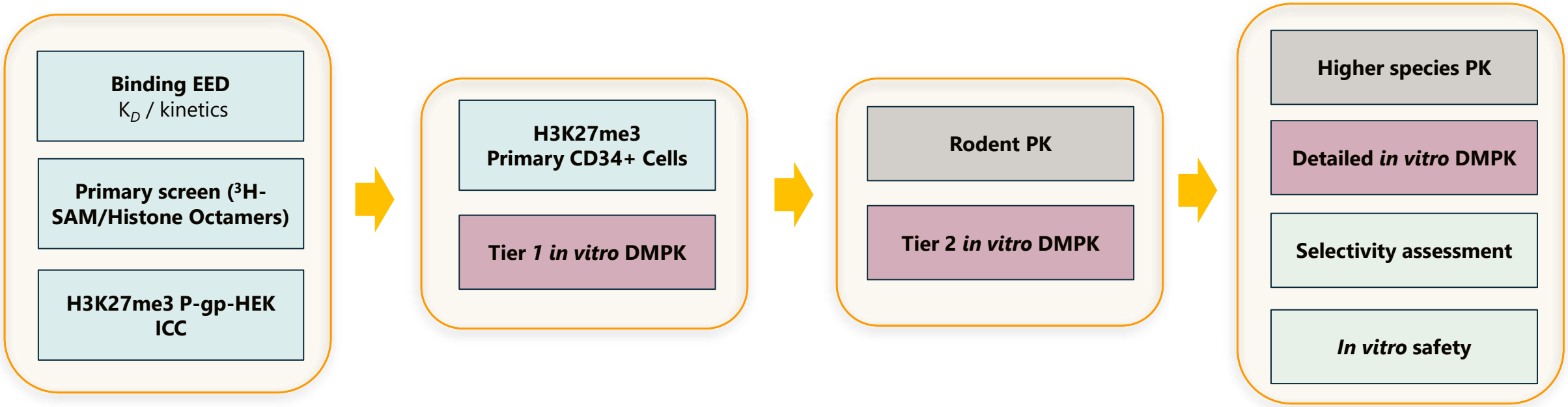

EED K_D (SPR) = 0.163 nM
biochemical IC_{50} (PRC2) < 5 nM
H3K27me3 IC_{50} (P-gp HEK) = 12 nM

HbF HUDEP2 EC_{50} = 29 nM
HbF CD34+ EC_{50} = 60 nM

LogD (pH 7.4) = 2.6
MDCK AB = 10.4 x 10^{-6} cm/s
HLM Clint = 16.2 uL/min/mg

HHEP Clint < 6.4 uL/min/mill cells
hPPB Fu = 22.2%
No inhibition of 5 CYPs at 10 uM
MDR BA/AB = 12.4
Mouse brain/plasma < 0.6%

No CYP3A4 TDI
Not AO substrate
IVMN – negative
Mini-Ames – negative
hERG inhibition < 10% at 10 uM
✓CEREP Safety-44 panel
✓KinaseProfiler™ panel (58 kinases)
✓Methyltransferase panel (26 enzymes)
✓Hepatotox assay (HepaRG spheroids)

FTX-6058 induces potent HbF induction in both HU responsive and non-responsive CD34+ cells from healthy donors

HU Non-responsive

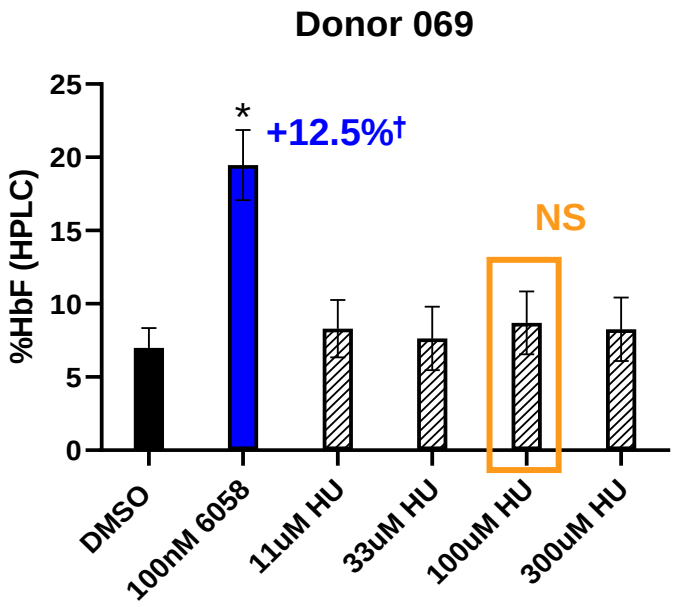

HU Responsive

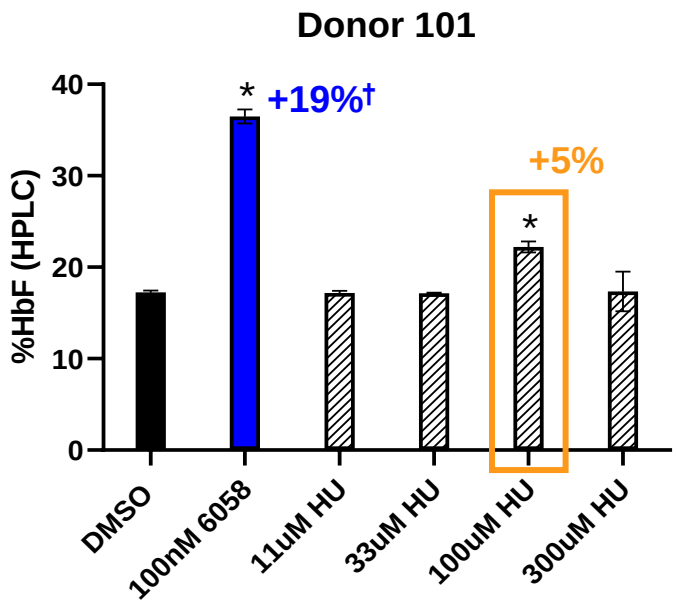

Partial HU Response

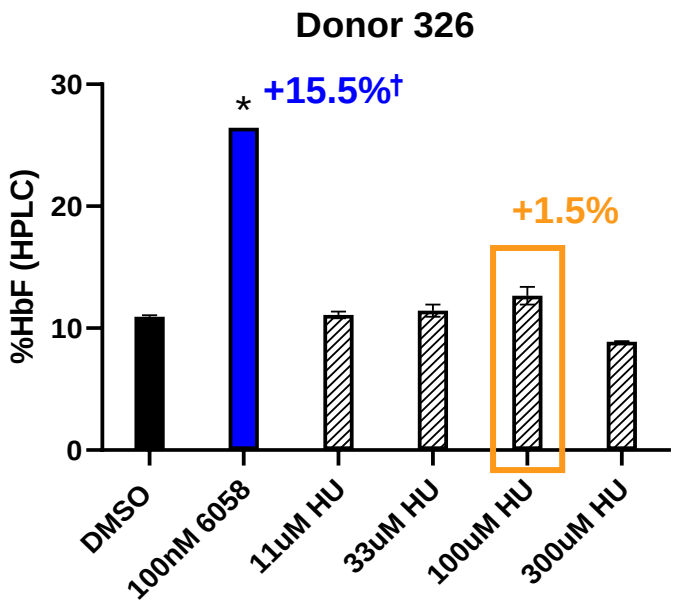

NS: Not significant; HU: Hydroxyurea; Fulcrum generated data; * p<0.05 one-way ANOVA in comparison to DMSO;
† Absolute increase in %HbF FTX-6058 vs. DMSO

FTX-6058 robustly induces fetal hemoglobin in CD34+ cells from healthy and SCD donors

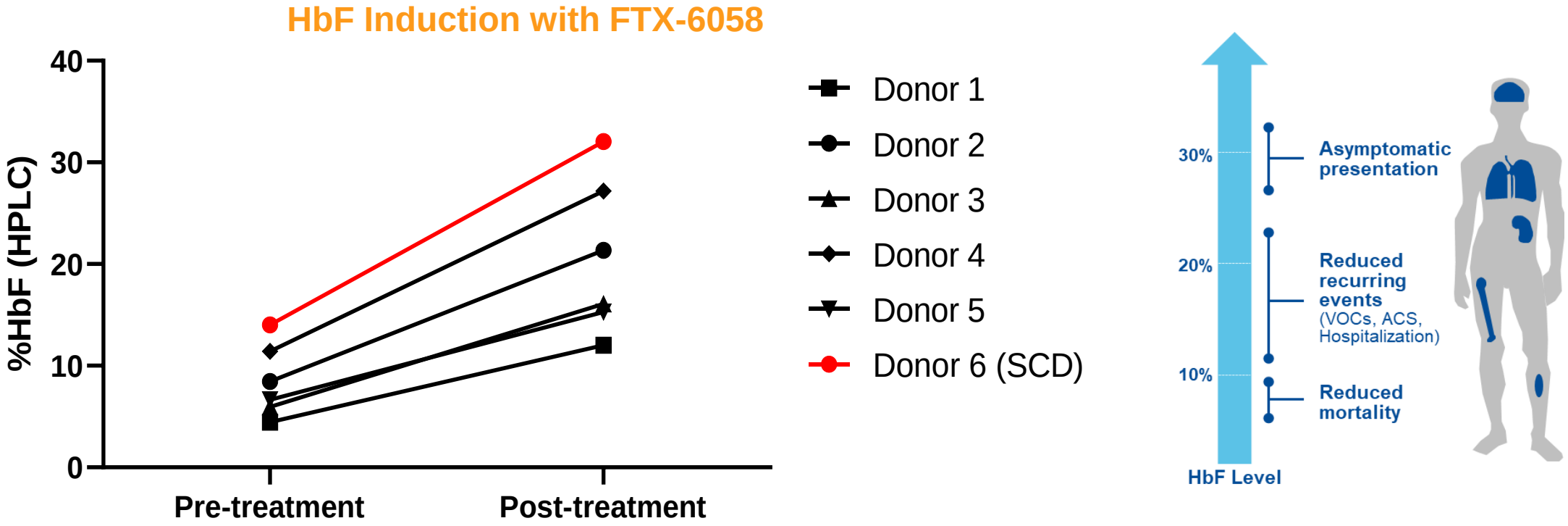

- Observe an absolute 8 – 18% increase in HbF upon treatment with FTX-6058, which has the potential to address mortality risk and recurring events in SCD patients
- Even small increases in HbF (1 – 5%) have the potential to provide clinical benefits to SCD patients

Powars, DR. Blood. 1984; Platt, OS. NEJM. 1994; Akinsheye, I. Blood. 2011; Fulcrum generated data.

FTX-6058 induces pancellular distribution of HbF

Left: pancellular HbF distribution in blood of patient with HPFH & SCD - asymptomatic SCD

HbF: ~30%

HbF: ~11%

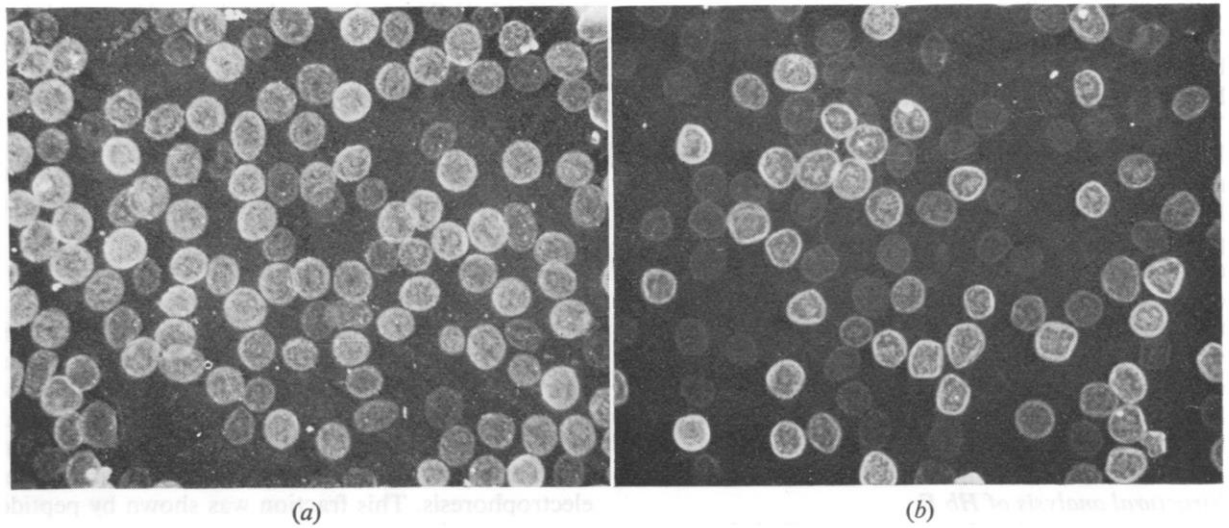

(a) (b)

Fig. 2 *Peripheral blood smears from (a) the propositus M.K. and (b) his mother S.C., stained with FITC labelled anti Hb F antibodies, demonstrating in the former that virtually all the cells are stained, but with considerable intercellular heterogeneity, while in the latter, two distinct populations are evident.*

Wood W. G. *et al.* J. Med. Gen. *1977,* **14,** 237.

FTX-6058 induced pancellular distribution of HbF

DMSO

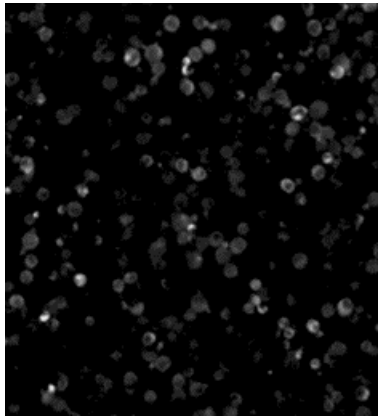

100 nM FTX-6058

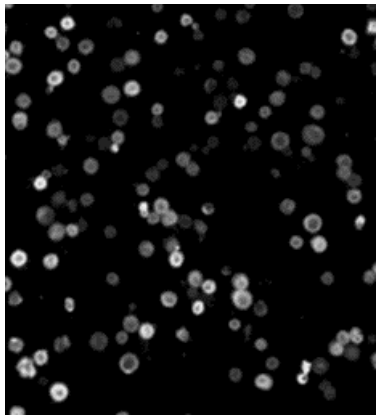

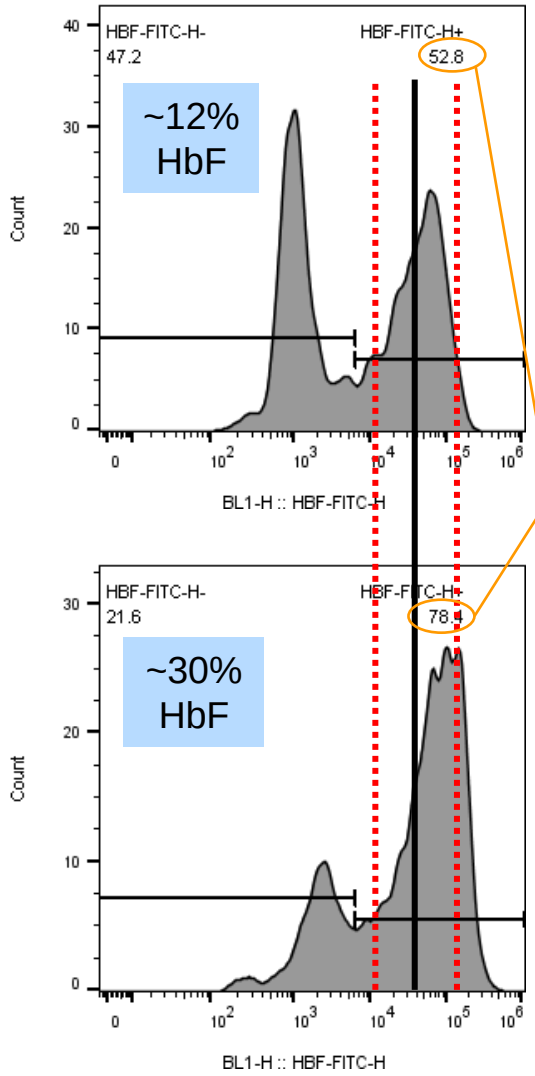

From 50% to 80% HbF^{hi}

HbF flow cytometry: CD34+ cells differentiated and treated for 7 days; Gated and quantified for HbF+/CD235a+/CD71+

Dose-dependent target engagement in the bone marrow of WT mice

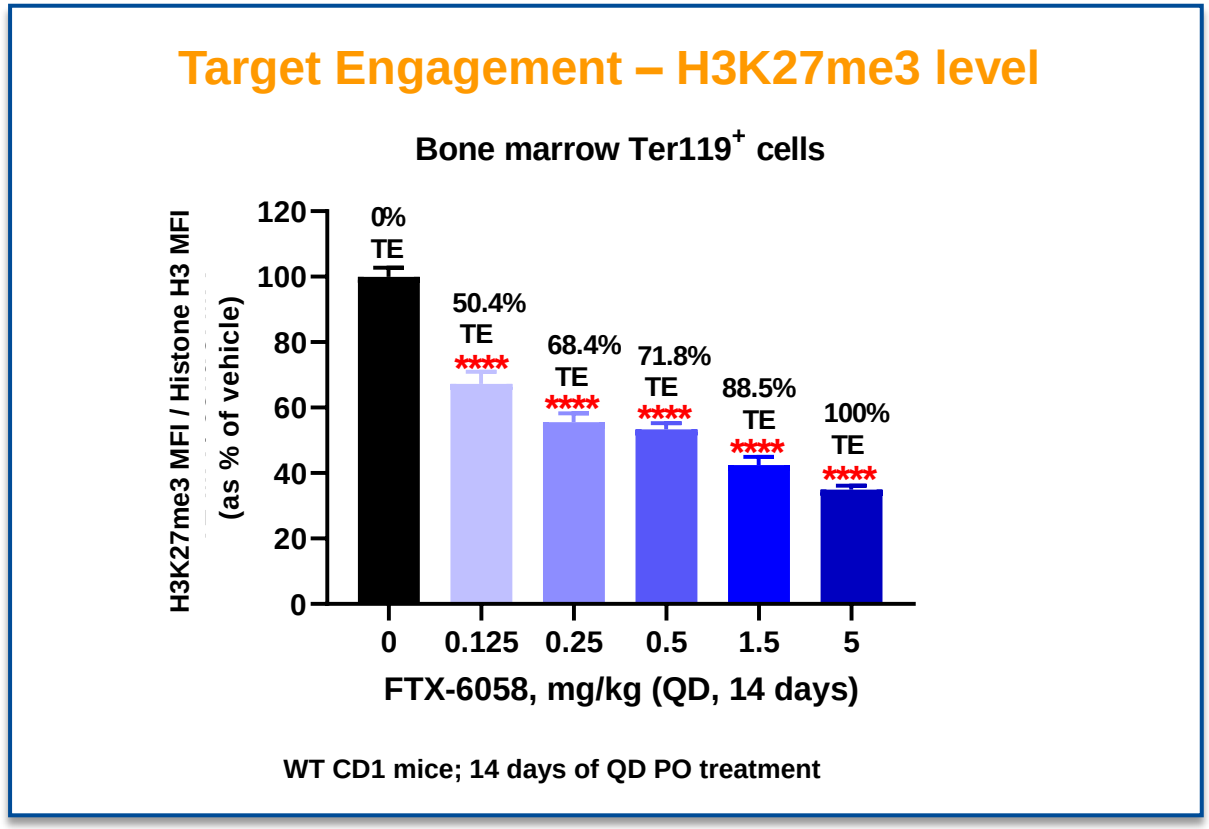

- Significant TE detected with QD dosing as low as 0.125 mg/kg
- TE of 80% as an anchoring parameter in design of Phase 1 clinical trial

FTX-6058 Induces HbF and Increases F-cells in the SCD Townes Mouse Model

Robust Target Engagement

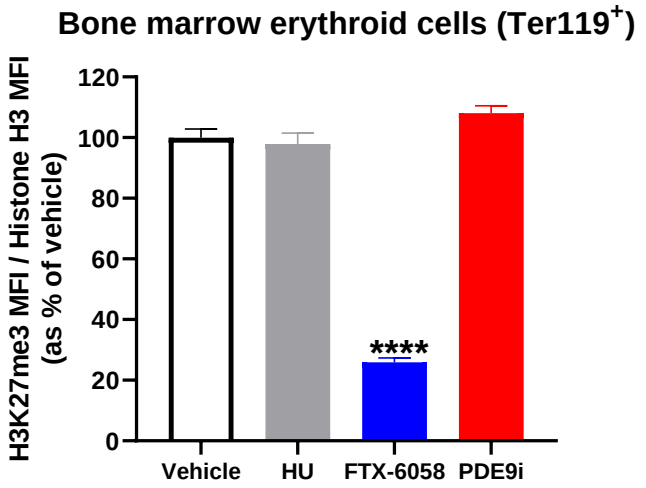

Increased F-cells (Flow Cytometry)

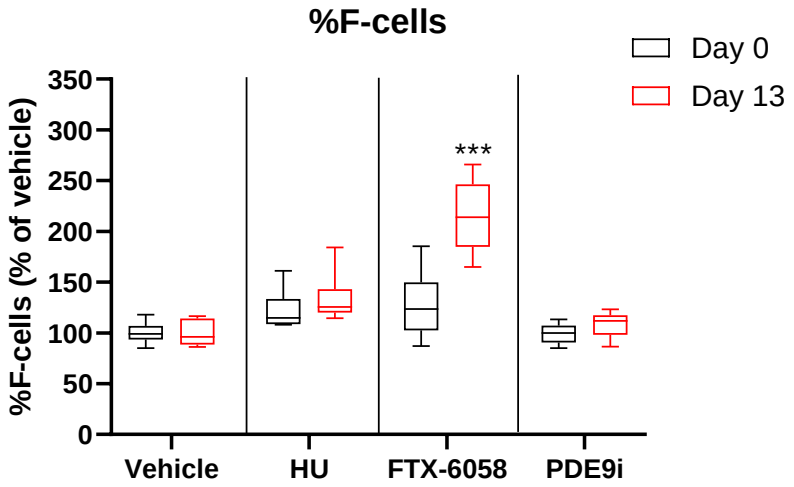

HbF Induction (HPLC)

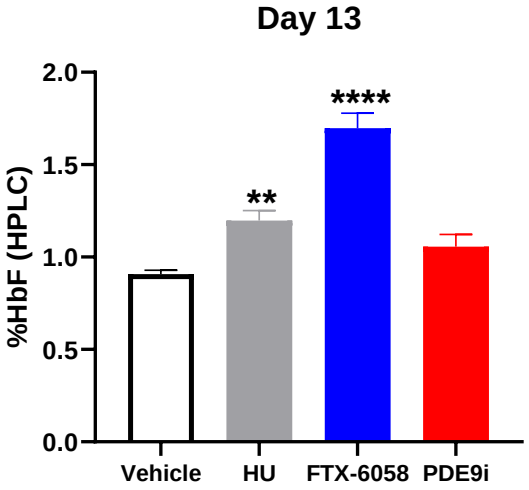

- Observe 3-fold increase in HbF mRNA (HBG1) levels with FTX-6058
- Maximal target engagement maintains ~30% of H3K27me3 mark

Fulcrum generated data; Townes SCD mice were orally dosed (QD) with vehicle, HU (100 mg/kg), FTX-6058 (5 mg/kg) or PDE9i (30mg/kg).
** p<0.01, *** p<0.001, **** p<0.0001, one-way ANOVA in comparison to pre-dose (Day 0) level (%F-cells) or vehicle group (target engagement and %HbF)

Time- and dose-dependent increase in relevant parameters in Townes SCD mice with QD dosing

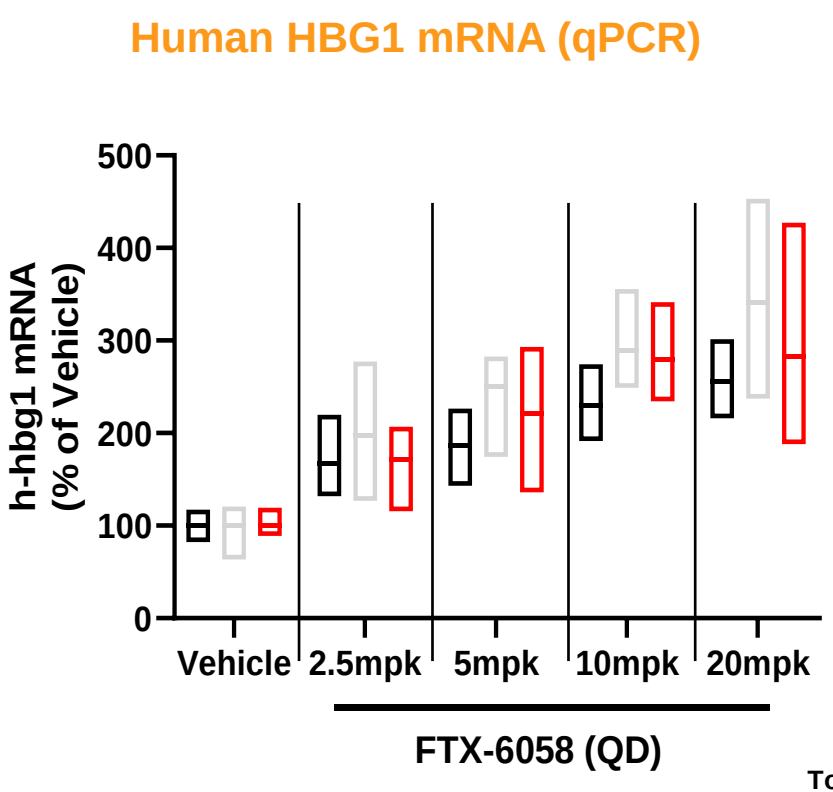

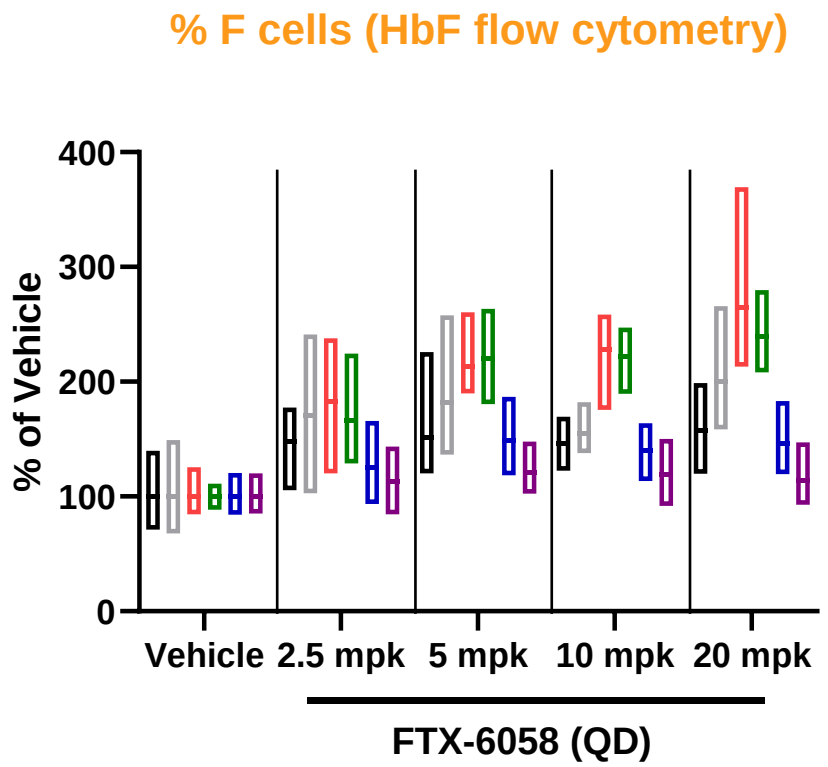

Townes mouse model (28 days treatment):
FTX-6058 was administered once per day at the indicated dose

- HbF elevation detected with QD dosing as low as 2.5 mg/kg
- Durable effect still observed 4 days post last dose

FTX-6058 male beagle dog PK

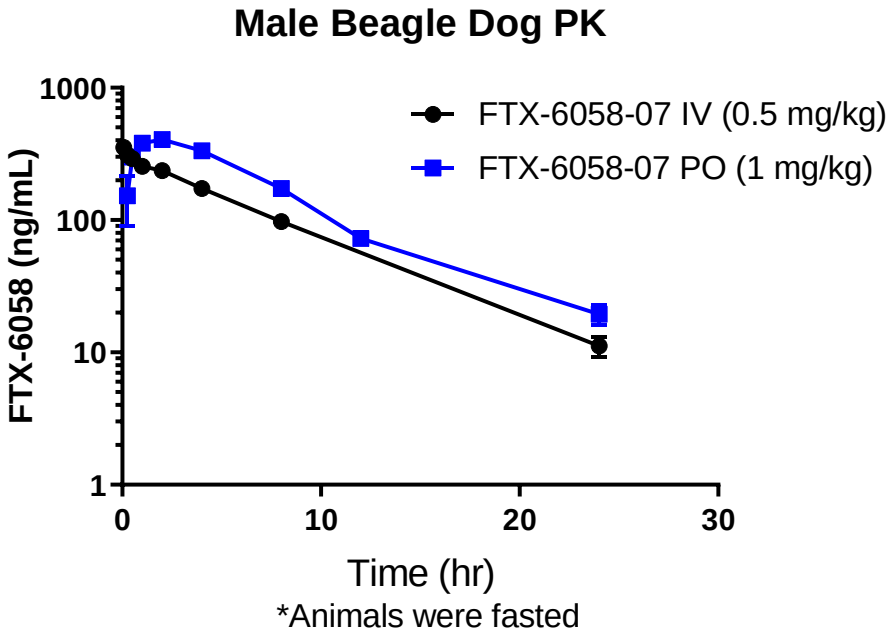

*Animals were fasted

- Good clearance IVIVC within preclinical species
- Reproducible PK between amorphous and crystalline forms
- Preclinical PK studies resulted in high confidence human PK projection
- *In vivo* PK data support progression of FTX-6058 to the clinic

ROA	Dose (mg/kg)	AUC_{inf} (ng.h/mL)	Cmax or C_0 (ng/mL)	Tmax (hr)	$T_{1/2}$ (hr)	Cl (mL/min/kg)	Vdss (L/kg)	%F
IV	0.5	2450	379		5.05	**3.41 (11.0% HBF)**	**1.30**	
PO	1	**3591**	413	1.67	**5.31**			**73.3%**

HBF – hepatic blood flow

Human dose simulations

- Target exposure (AUCtau: 73 h*ng/mL) at TE_{80} dose (1 mg/kg, PO, QD) in mice
- CLp predicted in humans using IVIVE and the geo mean of all allometric methods is convergent and values are similar; **the predicted human CLp of 8.4 mL/min/kg is moderate (~30% hepatic blood flow)**
- Several allometric methods were applied to estimate the human Vss; **the human predicted Vss of 2.2 L/kg is moderate**, greater than the volume of total body water
- **Assuming a 1-compartment model, the human $t_{1/2}$ is 3 hrs**
- Using statistical moments, the rate constant of absorption (ka) was similar across species (ranging 0.39-0.88 hr^{-1}); **the estimated k_a in humans is 0.65 hr^{-1}, indicating that absorption rate is slow-to-moderate**
- **The human oral F was predicted to be moderate, with a value of 60%**
- Using AUC as the PK parameter to be targeted for efficacy, **the predicted human oral dose is 4 mg QD**

Human dose projection by Leanne Bedard (Bedard ADME-Tox Solutions)

Early SAD PK from healthy volunteer study

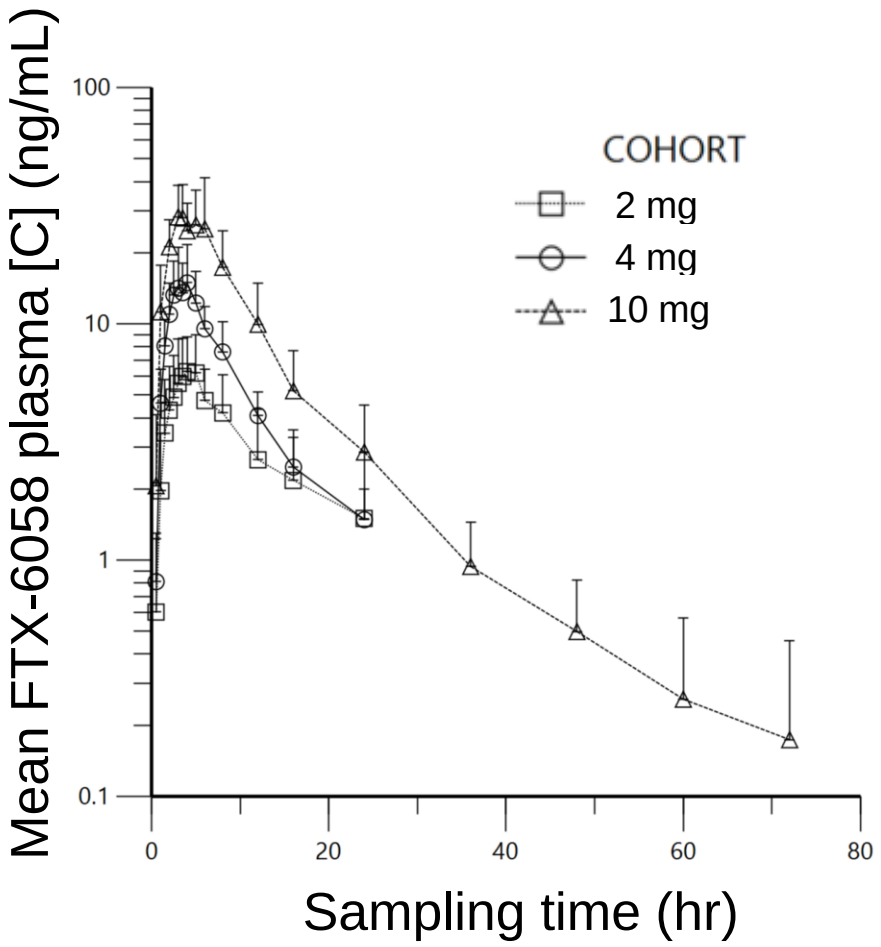

- Predictable linear progression in mean peak concentrations and exposures in dose escalation from 2 to 4 to 10 mg
- The observed human oral PK parameters align well with the predicted values (within 2-fold)
- Observed $t_{1/2}$ is longer than predicted, still supporting QD administration

PK Parameter	Dose = 10 mg		
	Observed	Predicted	Obs/Pred
C_{max} (ng/mL)	28.6	39	**0.73**
T_{max} (hrs)	3.76	2.5	**1.5**
AUC_{0-24} (ng hr/mL)	265	170	**1.6**
$t_{1/2}$ (hrs)	6.72	3.0	**2.2**

FTX-6058 has the potential to become a transformative therapy in SCD

Robust Preclinical HbF Induction May Translate to Meaningful Clinical Benefits

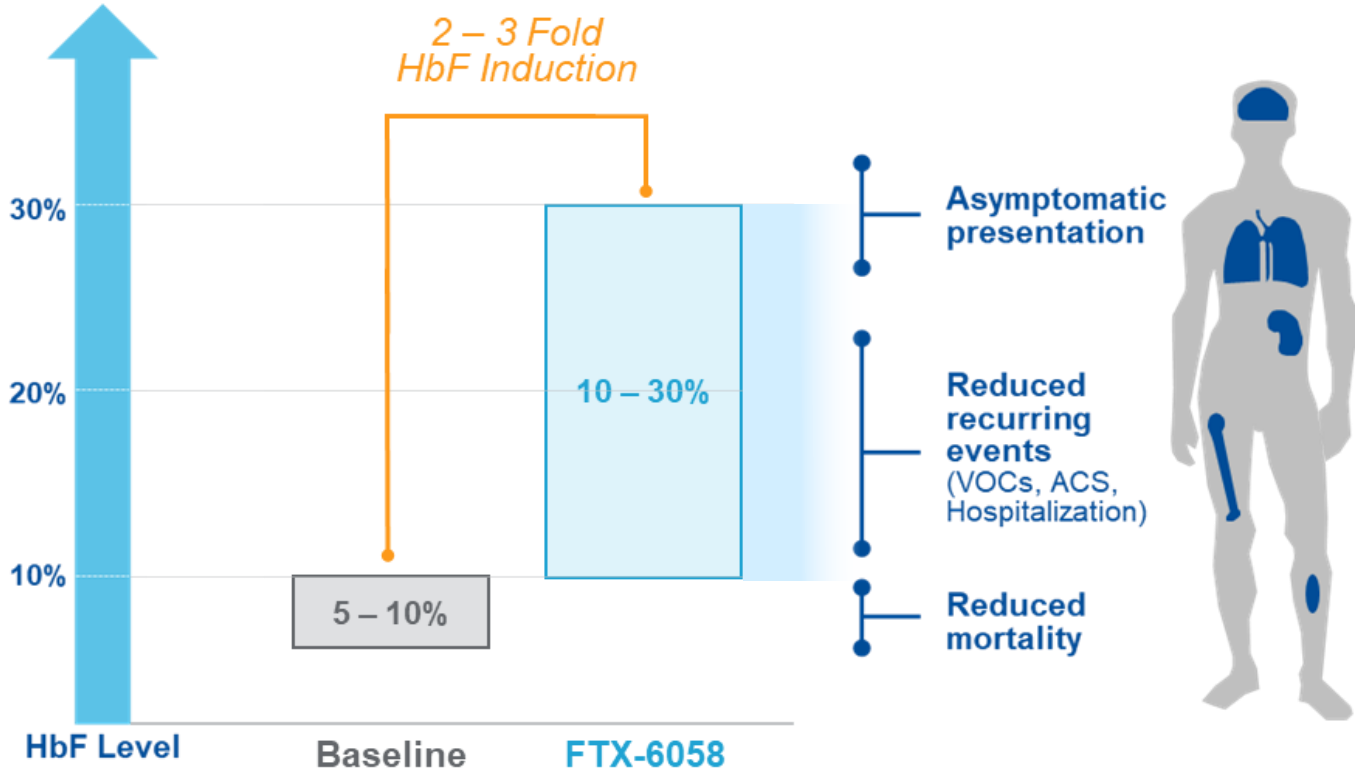

- EED Target identified with Fulcrum Product Engine
- Developed FTX-6058, a potent and selective EED-targeting PRC2 inhibitor
- Oral, once-daily dosing supported by PK and human dose projections
- Impressive pharmacological profile, with potential to be a disease-modifying therapeutic
- Composition of matter patent issued (expires in 2038)

- **Actively enrolling healthy volunteers in Phase 1 SAD/MAD studies**

Powars, DR. Blood. 1984; Platt, OS. NEJM. 1994; Akinsheye, I. Blood. 2011.

Acknowledgements

Chemistry	*In vitro* Biology	*In vivo* PK and pharmacology	Candidate progression and clinical data
Yanfei Dong (WuXi)	Kingsley Kofi Appiah	Leanne Bedard DMPK Solutions	David Peters
Shawn D. Johnstone (IntelliSyn)	Angela Cacace	David Eyerman	Kim Stickland
Steven Kazmirski	Michael Cameron	Christopher Moxham	William G. Tracewell (Nuventra)
Qingyi Li	Deena Qadir	Mark Roth	
Steven Mennen	Peter Rahl	Serena Silver	
Lorin A. Thompson, III	Billy Stuart	Keqiang Xie	
Owen B. Wallace			
Yifeng Zhao (WuXi)			
Feng Zhou (IntelliSyn)			

Fulcrum Therapeutics

Fulcrum Therapeutics | 26 Landsdowne Street, 5th Floor | Cambridge, MA 02139 | fulcrumtx.com